EJECTOR DRIVEN REFRIGERATION SYSTEMS

SAMUEL DEVRAJ ARULMANI

NATIONAL UNIVERSITY OF SINGAPORE

2012

EJECTOR DRIVEN REFRIGERATION SYSTEMS

SAMUEL DEVRAJ ARULMANI

(B.E.), Anna University

A THESIS SUBMITTED

FOR THE DEGREE OF MASTER OF ENGINEERING

DEPARTMENT OF MECHANICAL ENGINEERING

NATIONAL UNIVERSITY OF SINGAPORE

2012

ACKNOWLEGEMENTS

TABLE OF CONTENTS

SUMMARY

Ejector Driven Refrigeration Systems

(January 2012)

Samuel Devraj Arulmani, B.E., Anna University

Supervisor: Asst. Prof. Chua Kian Jon, Ernest

Co-supervisor: Prof. Chou, Siaw Kiang

Ejector driven systems, wherein an ejector is used as a thermal compressor are a viable alternative to traditional vapour compression refrigeration systems since they are simple to construct, operate and maintain. However their popularity has been limited by low COP and small operating windows. This project is aimed at trying to improve the performance of these systems so as to make them more attractive.

The associated work carried out is reported as follows;

1. **Introduction and Literature Review**

   A comprehensive study to understand the progress in research carried out so far was conducted. From the study results, an introduction into the concepts of an ejector has been given and the relevant governing equations have been discussed.

2. **Traditional Ejector Model Development**

   A 1D model was developed in MATLAB to predict the performance of the ejector using conservation laws. The model helps to understand the working of an ejector and to predict the performance for different geometries and operating conditions.

3. **Alternate Refrigerant Prediction for Existing Ejector Systems**

   Most of the ejector systems currently in operation use refrigerants which have high Global Warming or Ozone Depletion Potential. The validated 1D model is used to propose suitable alternate environment-friendly refrigerants for existing ejector systems currently using older refrigerants. Base refrigerants considered are R11, R123 and R141b. Replacement refrigerants analysed are R134a, R245fa, R245ca, Water (H_2O) and Ammonia (NH_3).

   In general, ammonia and R134a develop a much higher entrainment than the base refrigerants. However they also have high operating pressures. R245fa and R245ca have operating pressure ranges very close to those of the base refrigerants. But their entrainments are often slightly lesser than those of the base refrigerants.

4. **The Roto Ejector Concept and Model Development**

   The Traditional Ejector model has then been modified to simulate the performance of a novel "Roto-dynamic Ejector". The developed model is used to compute the expected performance for different refrigerants.

5. **Comparison of Traditional and Roto-Ejector performances**

   The Traditional and Roto Ejector model performances are compared and improvements are gauged. It is observed that incorporating a Roto-ejector can improve the COP of a system up to 30% over that of the traditional ejector. The Entrainment ratio is also increased by 12 – 29%. Based on the results, conditions for optimal operation are proposed.

LIST OF FIGURES

LIST OF TABLES

LIST OF SYMBOLS

1D	One Dimensional
2D	Two Dimensional
3D	Three Dimensional
A	Cross Sectional Area
AR	Area Ratio $\left[\frac{A_t}{A_k}\right]$
CFC	Chloro-Fluoro-Carbon
CFD	Computational Fluid Dynamics
COP	Coefficient of Performance
C_p	Specific heat at constant pressure
C_v	Specific heat at constant volume
EDRS	Ejector Driven Refrigeration System
g	Acceleration due to gravity (9.81 m /s^2)
GWP	Global Warming Potential
h	Enthalpy
HCFC	Hydro Chloro-Fluoro-Carbon
m	Mass flow rate
M	Mach number
MATLAB	A computing language developed by MathWorks
NXP	Nozzle Exit Position
ODP	Ozone Depletion Potential
P	Pressure
Q	Heat Input
r	Blade radius from centreline

REFPROP   A Computer program developed by National Institute of Standards and Technology (NIST) to calculate refrigerant and mixture properties

RERS   Roto- Ejector Refrigeration System

T   Temperature

U   Velocity of Rotor blade

V   Absolute Velocity of flow

VCRS   Vapour Compression Refrigeration System

W   Work Done

α Angle between rotor axial and relative flow directions at inlet

β Angle between rotor axial and relative flow directions at outlet

γ Ratio of Specific heats (C_p / C_v)

θ Angle between rotor axial and absolute flow direction at inlet

ΔP Pressure lift

Φ Angle between rotor axial and absolute flow direction at outlet

ρ Density

ω Entrainment ratio (m_s / m_p)

Subscripts

1   Ejector Primary fluid inlet

2   Ejector Outlet

3   Condenser Inlet

4   Expansion Valve Inlet

5   Evaporator Inlet

6	Ejector Secondary fluid inlet
2^1	Compressor Inlet
c	Condenser
cr	Critical conditions
e	Evaporator
g	Generator
i	Start of constant pressure mixing section
i^1	Primary nozzle exit before turbine rotor
j	Start of constant area mixing section
k	Start of diffuser section
m	Mixing section
o	Stagnation conditions
p	primary fluid
s	secondary fluid
t	throat section

CHAPTER I

INTRODUCTION AND LITERATURE REVIEW

1.1   INTRODUCTION

An ejector is a device which utilizes a high momentum primary fluid to entrain a low pressure secondary fluid. Both the fluids then mix together in a constant area section and are compressed to an intermediate pressure in a diffuser.

Among the various functions for which an Ejector-driven system can be employed is that of replacing or complementing the compressor in a traditional vapour-compression refrigeration system. Such a system has the advantage of being uncomplicated, inexpensive and maintenance free since it does not have any moving components. It also results in substantial power savings as the compressor can be greatly reduced in size or eliminated altogether.

However, these systems are not widely popular till-date because their range of operation is limited and the Coefficient of Performance (COP) is very low. Contemporary research in this area is therefore focussed on eliminating these drawbacks to ensure a wider acceptance of these devices.

1.2   LITERATURE REVIEW

Ejectors have been used in engineering applications since the early 1900s. The device was invented by Sir Charles Parsons in 1901 and initially used in steam related

applications. They were introduced into air-conditioning applications later on and were very popular in the 1930s when developments to these systems reached a standstill as mechanical compressors were introduced. Studies on ejectors were revived in the 1990s as awareness about Global Warming and Ozone layer Depletion increased and efforts were made to make systems more environment-friendly.

In 1950, Keenan and Neumann [1] presented the first comprehensive theoretical and experimental study on Ejectors. Their results have the distinction of being used as the basis for ejector design and analysis in almost all the subsequent researches.

Two established techniques are used for modelling ejectors – The constant pressure model and the constant area model. Sun and Eames [2] showed that the constant pressure model has better performance. Then in 1996, going a step further, they proposed a one dimensional (1D) method to calculate the optimum area and entrainment ratios if the inlet and outlet conditions are specified. The primary and secondary fluids were assumed to have the same molecular weight and ratio of specific heats. Stagnation conditions were imposed at the inlet and exit.

In 1999, Huang and Chang [3] proposed a modified 1D analysis method by assuming a hypothetical throat in the constant area section of the ejector. Experiments to compare the model's performance were then carried out for R141b refrigerant.

Sriveerakul et al. [4, 5] and Pianthong et al. [6] used CFD to predict and optimise the performance of ejectors. Steam was used as the fluid. They also compared results

obtained by 2D and 3D Ejector models and concluded that complex 3D models are not required for basic ejector simulations.

Some recent studies have also focussed on ejectors which handle two phase fluids as a means to improve on the basic cycle performance. Chaiwongsa and Wongwises [7] proposed using the ejector as an expansion device and eliminating the expansion valve to improve the cycle efficiency. Menegay and Kornhauser [8] investigated the performance of a similar cycle and proposed that the theoretical COP can be improved up to 21% under certain conditions. Sarkar [9] carried out thermodynamic analysis on certain natural refrigerants to optimise geometric parameters for maximum COP and performance improvement.

Other research efforts at geometric parameter optimisation encountered include that by Zare- Behtash et al [10] who examined the effect of primary jet geometry on ejector performance using high-speed schlieren photography and determined that circular nozzles provide better performance than nozzles of other shapes like elliptical or square. Ruangtrakoon et al [11] experimentally examined the effect of primary nozzle throat dimensions and exit mach numbers on the ejector performance and the system COP. However they strongly recommended that a CFD study be conducted in tandem with experiments to determine the process inside the ejector. Cizungu et al [12] modelled and optimised two phase ejectors with a control volume approach and concluded that the dimensions of the ejector configuration play a dominant role in deciding the optimum range of performance of the ejector.

Another strategy normally adopted for cycle performance improvement is coupling the basic ejector cycle with an allied cycle. Huang et al [13, 14] used ejectors to complement the performance of a solar assisted heating / cooling system. They concluded that ejectors can handle around 17 – 27% of the cooling load of the system by simulating for long term performance. Diaconu [15] carried out energy analysis of a system where ejectors assist the solar cycle to compensate for fluctuations in availability of solar power. The author then defined energy efficiency parameters to determine the optimum system configuration. Wang and Shen [16] carried out energy analysis on a novel solar bi ejector system where the circulating pump is replaced by an injector and concluded that there exists an optimum generation temperature, at which the overall energy and energy efficiencies are both maximum and the total energy loss is minimum. They also pointed directions for optimizing the system.

Researchers like Elbel [17] proposed using ejectors to improve expansion work in trans-critical systems which typically have large throttling losses. After carrying out system and component level investigations, he claims a COP and cooling capacity improvement of up to 18% can be achieved for refrigerants like R744 by replacing the conventional expansion valve with an ejector.

Other strategies adopted for performance improvement of ejectors include providing a bell mouthed entry at the nozzle, superheating the primary and entrained fluids and using refrigerants which have a bell shaped saturation curve (Huang [18])

The first commercial ejector system in recent times is probably that developed by Denso Corporation for use in cold storage trucks as a follow up to their patents US 6438993 [19] , US 6935421 [20] , US 7254961 [21] and a few others.

1.3 NOVELTY OF THIS RESEARCH

Based on the literature review carried out, it is understood that the existing research on Ejector Driven systems has been focussed on

1. Predicting the flow phenomena inside the ejector and developing computational models

2. Optimising the ejector performance by geometric or operating parameter optimisation.

3. Improving the ejector performance by using new age refrigerants and refrigerant mixtures or by using the ejector with allied cycles like solar or trans-critical systems.

None of the researchers so far have dealt with "Alternate Refrigerant Prediction" for existing ejector systems. A study addressing this issue is important as most ejector systems currently studied in researches or that which exist in operation are those that have been designed for CFCs and HCFCs which are now banned / restricted. An alternate refrigerant prediction study would help to determine the best environment friendly alternate. It would also help to determine the expected changes in the system performance due to the refrigerant change.

This is one of the objectives of the thesis. A model has been developed to predict environment friendly alternates for banned / phased out refrigerants. Once the geometries of the existing ejector system are fed into the model, the expected performance of the system can be computed. Any refrigerant in the REFPROP database can be designated as the base refrigerant or the target refrigerant and its performance computed.

The other issue addressed in this thesis is "Performance Improvement of the Ejector Cycle". As specified at the start of this section, researchers throughout the world have attempted to improve the performance of the ejector by adjusting the geometric parameters, using new age refrigerants and mixtures or by combining the ejector cycle with an alternate cycle. Stepping away from all these previous approaches, to achieve performance improvement, we introduce a novel component called the "Roto-dynamic Ejector". It is a component, similar to a turbine driven compressor, designed to utilize the flow energy of the high velocity fluid at primary nozzle exit to increase the pressure of the entrained secondary fluid along with the primary fluid. It prevents the energy loss due to turbulent dissipation which normally occurs in ejectors and hence operates at high levels of efficiency. A model has been developed based on the concerned governing equations. The performance of the model has then been compared with that of the basic Ejector Driven and Vapour Compression cycles and the improvements have been discussed.

The roto-dynamic ejector is a new concept which has never been explored by researchers before. However it is heartening to note from the results obtained from

our built up model that this could be a new avenue for productive research in the field of ejectors.

1.4   SCOPE OF WORK

The work carried out for this thesis is described in the following sections.

1. Traditional Ejector Model Development

    A 1D model has been developed in MATLAB to predict the performance of the ejector using conservation laws. The model helps to understand the working of an ejector and to predict the performance for different geometries and operating conditions.

2. Alternate Refrigerant Prediction for Existing Ejector Systems

    A validated 1D model has been used to predict suitable alternate environment-friendly refrigerants for existing ejector systems currently using older refrigerants. Though results for only certain refrigerants are shown, similar predictions can be made for any refrigerant in the REFPROP database.

3. The Roto Ejector Concept and Model Development

    The Traditional Ejector model has then been modified to simulate the performance of a Roto Ejector. The model is used to compute the improved performance over the traditional Ejector driven and Vapour Compression systems.

4. Comparison of Results and Discussion

    This section is divided into two sub sections. Firstly, alternate refrigerant comparisons are made. In addition, for a given base refrigerant, the steps involved in selecting the best alternate refrigerant are discussed. Secondly, the

traditional and Roto-Ejector model performances are compared and

improvements are gauged. Conditions for optimal operation are then laid out.

1.5   ARRANGEMENT OF THE THESIS

Chapter I of this thesis gives a general introduction of the topic. A comprehensive literature review of the work carried out by previous researchers is done and the research directions adopted are highlighted. The novelty of this work and the scope of the thesis are then mentioned.

Chapter II gives a technical introduction into the concepts of an ejector. The different parts of an ejector, the governing equations involved and the variation of the fluid properties as it flows along the ejector are specified. The drawbacks of using the ejector in its basic form are revealed and the configurations adopted for improving the performance are discussed. The final section focuses on the concept of the Roto-Ejector and gives some insight into the background of this development.

Chapter III gives information about the 1D model developed for traditional ejector performance. The assumptions involved, the governing equations used and the computational procedure adopted are explicitly mentioned.

Chapter IV deals with results and discussion. The model laid out in Chapter III is first validated with available experimental data from the literature. It is then used to suggest refrigerant replacement options for existing systems using phased-out

refrigerants. The merits and demerits of each replacement considered are then discussed.

Chapter V outlines the roto-ejector concept, the dynamics of operation and the model developed to simulate its performance. It also compares the performance of the roto-ejector with the traditional ejector and elaborates on the improvements achieved.

Chapter VI gives a summary of the results and useful conclusions drawn from the previous chapters. A section on the recommendations for future work is also included.

CHAPTER II

BASIC EJECTOR DRIVEN SYSTEMS

2.1   A TYPICAL EJECTOR DRIVEN REFRIGERATION SYSTEM

Figure 2.1 shows the arrangement of a simple ejector-driven system for refrigeration or air-conditioning applications.
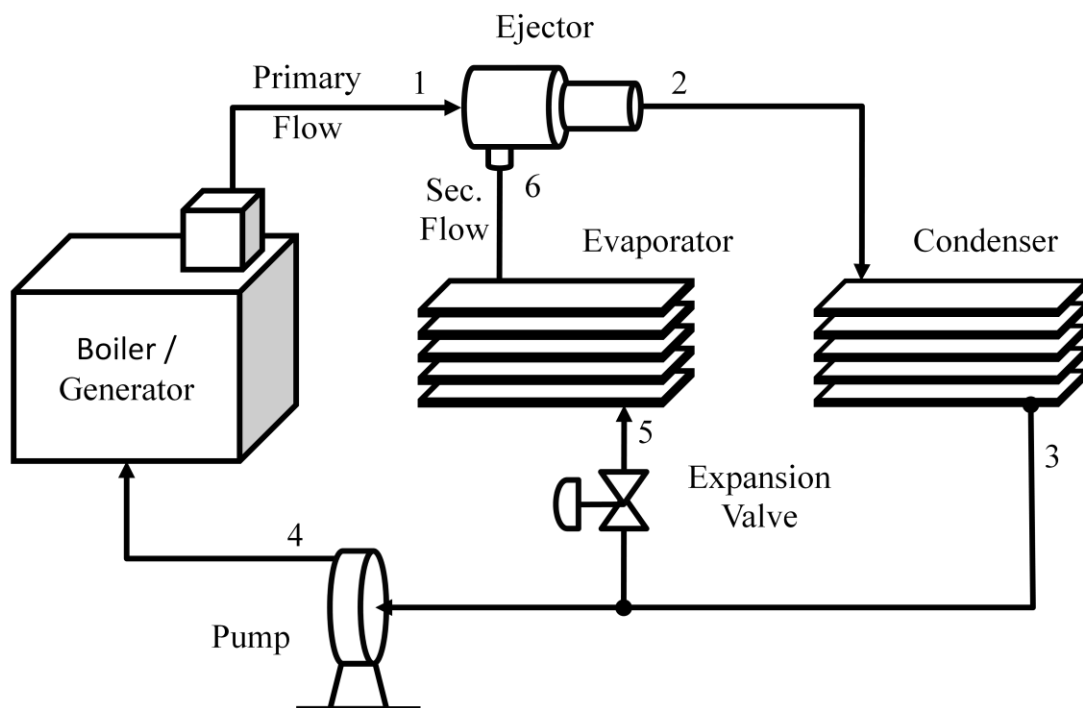
Figure 2.1 A Basic Ejector Refrigeration System

The heart of this setup is the Ejector. It is driven by waste heat from the Boiler/ Generator. This high momentum waste heat, also known as the "primary", then entrains a low pressure "secondary" fluid from the Evaporator. Both the fluids mix together in the ejector and leave at an intermediate pressure to the Condenser. At the outlet of the Condenser, the liquid and vapour phases are separated. The vapour is throttled in the Expansion Valve, producing a chilling effect, which is utilized in the

Evaporator. As the throttled vapour passes through the Evaporator, it absorbs heat from its surroundings. The hot fluid from the outlet of the Evaporator enters the Ejector as the secondary fluid and the cycle is repeated. The liquid from the Condenser is pumped to the Boiler/Generator, where it absorbs the waste heat and gets superheated as the primary fluid for the ejector.

Figure 2.2 shows the Pressure-Enthalpy (P-h) diagram for such a system
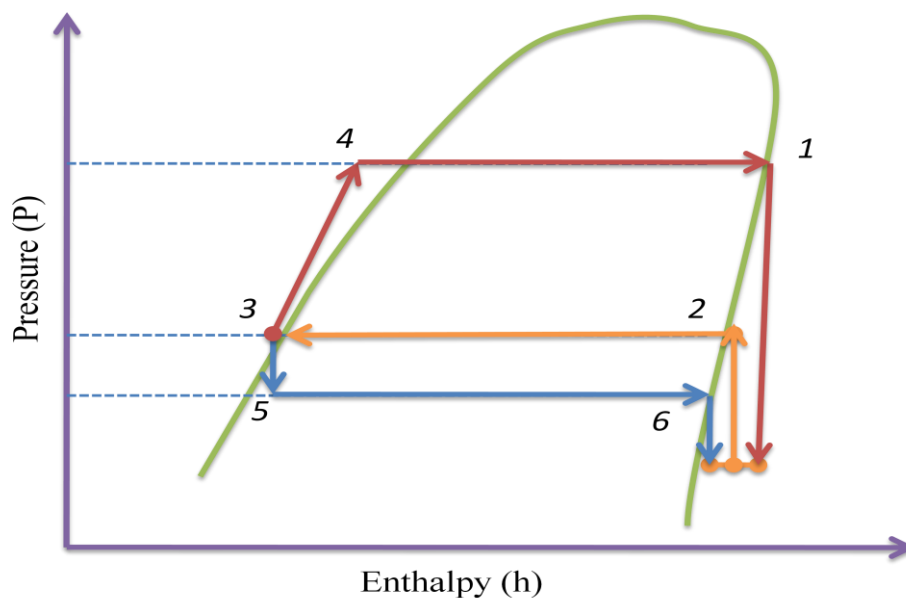
Figure 2.2 P-h diagram for an Ejector Driven Refrigeration System

The Primary fluid from the Boiler/Generator (4-1) is superheated or saturated and has a high pressure and temperature. The Secondary fluid from the Evaporator (5-6) is also superheated but at a lower pressure. Both these fluids mix in the Ejector and get compressed to an intermediate pressure. The Primary fluid expands from State 1 to 2, while the Secondary fluid is compressed from State 6 to 2. In the Condenser (2-3), the fluids are cooled while the pressure almost remains constant. At State point 3, the outlet of the condenser, the mixed streams are separated. One stream passes through the Expansion Valve (3-5) while the other is pumped back (3-4) to the

Boiler/Generator. To improve the efficiency of operation, an additional Pre-Cooler and Regenerator may be used though not necessary. The fluid throttled in the Expansion Valve absorbs the heat from the Evaporator (5-6) and again reaches a superheated or saturated state at Point 6.

Ideally, the operation in the Ejector and the pressure addition in the Pump are considered isentropic. The heat additions at the Boiler and Evaporator are considered as Constant Pressure heat additions. The heat rejection in the Condenser also occurs at constant pressure. The throttling in the Expansion Valve is isenthalpic.

2.2   INTERNALS OF A BASIC EJECTOR

Figure 2.3 shows the internals of a traditional ejector in its basic form.
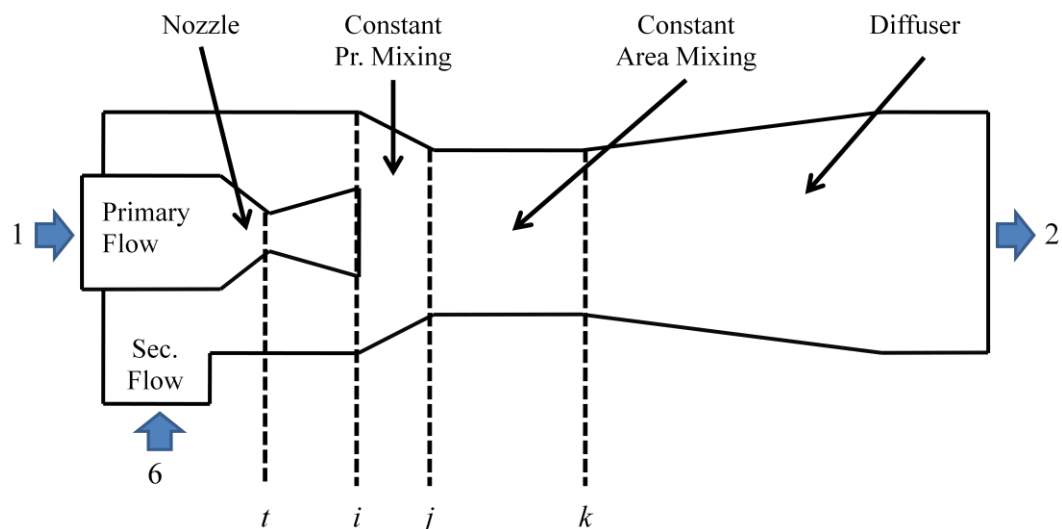
Figure 2.3 A typical Ejector

The major components are; Primary flow nozzle, Secondary flow entrainment chamber, Constant Pressure mixing section, Constant Area mixing section and Diffuser. The Primary fluid enters from the left at Point '1' and then expands in the nozzle to reach supersonic speeds at the exit Point 'i'. Here the pressure of the

Primary fluid drops below that of the Secondary fluid at '6' and so it entrains the Secondary fluid into the Mixing chamber. Both the fluids mix in the Constant Pressure and Area sections and shock to decelerate to subsonic speeds. In the Diffuser section, the mixture's pressure then increases as it flows towards the exit Point '2'.

Figure 2.4 shows the Pressure and Velocity characteristics of flow along the ejector.
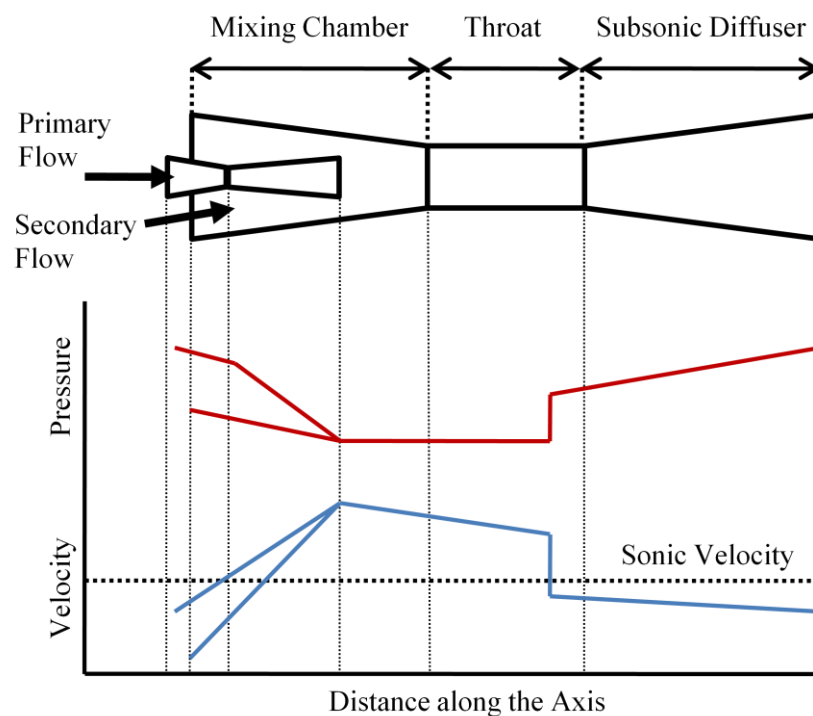
Figure 2.4: Flow characteristics along an Ejector

2.2.1   PRIMARY NOZZLE

The primary nozzle used is generally a convergent divergent nozzle (Figure 2.5) since supersonic flow at the exit of the nozzle is desired. At the inlet to the nozzle the fluid is subsonic and close to its stagnation conditions. The convergent portion of the nozzle accelerates the fluid as the cross sectional area available for the fluid decreases along its length.

Throat
Section

Inlet

Exit

Convergent
Section
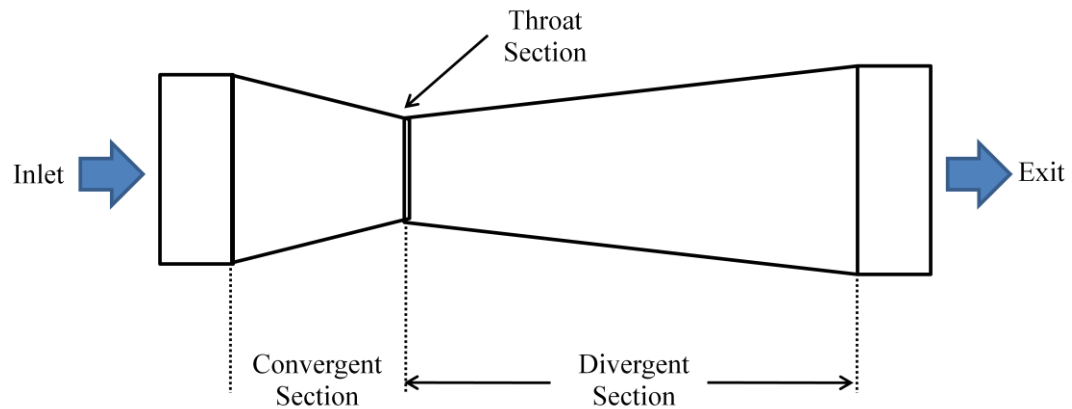
Divergent
Section

Figure 2.5: Cross section of a Convergent – Divergent nozzle

The downstream flow in the nozzle depends on the exit pressure. As the exit pressure is decreased, the flow characteristics change as described below. Figure 2.6 gives a pictorial representation of this phenomenon.

As the exit pressure is decreased, the flow accelerates as it flows through the convergent section. It reaches the maximum velocity at the throat. The velocity then decreases as it flows towards the exit. Curve *'i'* of Figure 2.6 represents this condition.

As the exit pressure is further decreased, the increases in flow rate and velocity are greater than that of curve '*i*' at the throat (curve '*ii*'). However the velocity still doesn't reach sonic conditions and the nozzle continues to behave like a venturi. Along the divergent section, the trend is the same as of curve '*i*'.

If the exit pressure is decreased to the nozzle critical pressure, the velocity of fluid reaches sonic conditions (Mach number = 1) at the throat. The flow is then said to be choked and the maximum flow rate has been achieved (curve '*iii*').

Decreasing the exit pressure further results in supersonic flow in the divergent portion
of the nozzle (curve '*iv*'). The nozzle is then operating at its optimum condition for
use in an ejector. The flow rate is maximum and choked. The flow is also supersonic
and very high velocities are obtained at the exit.
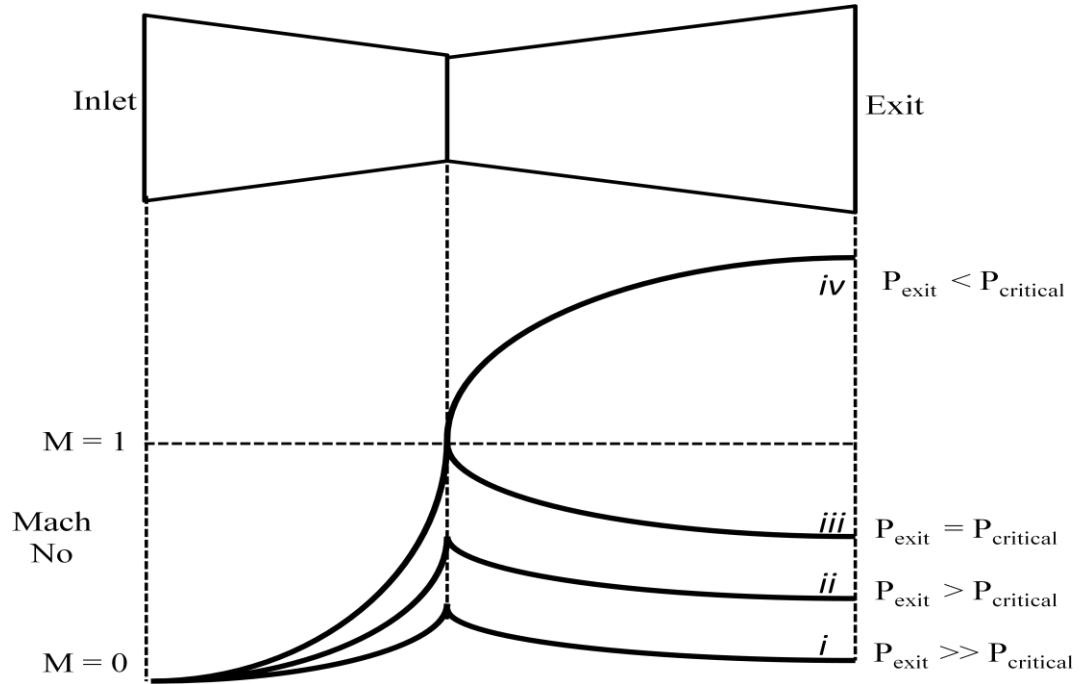
Figure 2.6: Choking phenomena in the Nozzle

The equations which govern the flow through a nozzle are shown below.

$$\frac{P}{P_0} = \left[1 + \left[\frac{\gamma - 1}{2}\right]M^2\right]^{-\left(\frac{\gamma}{\gamma-1}\right)} \tag{2.1}$$

$$\frac{T}{T_0} = \left[1 + \left[\frac{\gamma - 1}{2}\right]M^2\right]^{-1} \tag{2.2}$$

$$\frac{\rho}{\rho_0} = \left[1 + \left[\frac{\gamma - 1}{2}\right]M^2\right]^{-\left(\frac{1}{\gamma-1}\right)} \tag{2.3}$$

The critical conditions can be calculated by substituting the value of Mach number as unity in the above equations. We then get

$$\frac{P_{cr}}{P_0} = \left[\frac{2}{\gamma + 1}\right]^{\left(\frac{\gamma}{\gamma - 1}\right)} \tag{2.4}$$

$$\frac{T_{cr}}{T_0} = \frac{2}{\gamma + 1} \tag{2.5}$$

$$\frac{\rho_{cr}}{\rho_0} = \left[\frac{2}{\gamma + 1}\right]^{\left(\frac{1}{\gamma - 1}\right)} \tag{2.6}$$

For air, $\gamma = 1.4$. So $\frac{P_{cr}}{P_0} = 0.528$, $\frac{T_{cr}}{T_0} = 0.833$ and $\frac{\rho_{cr}}{\rho_0} = 0.634$

The critical mass flow rate can be calculated by

$$\dot{m}_{cr} = \rho_{cr}\ A_{cr}\ V_{cr} \tag{2.7}$$

The subscript 'cr' indicates critical conditions, for example A_{cr} is the cross sectional area at the throat and V_{cr} is the velocity of sound.

Two factors of the nozzle influence the overall ejector performance – The Nozzle design and Nozzle position. The effect of the nozzle position on the system COP was analysed by Chunnanond and Aphornratana [22]. The nozzles used were convergent-divergent ones with a circular cross section. The fluid used was steam but similar characteristics are expected for other fluids also. Their results are shown in the following Figure 2.7. The Zero nozzle position is defined as the point where the nozzle exit tip is in line with the constant area mixing chamber. A Positive (+) nozzle

position indicates the nozzle projects into the mixing chamber. A Negative (-) position indicates the nozzle is pulled away from the mixing section.

As the primary nozzle is moved away from the mixing section, the system COP obtained increases slightly. This is probably because then there is better mixing at constant pressure and constant area. When the primary nozzle protrudes into the constant area section, only constant area mixing is possible and subsequently the COP obtained is lesser.
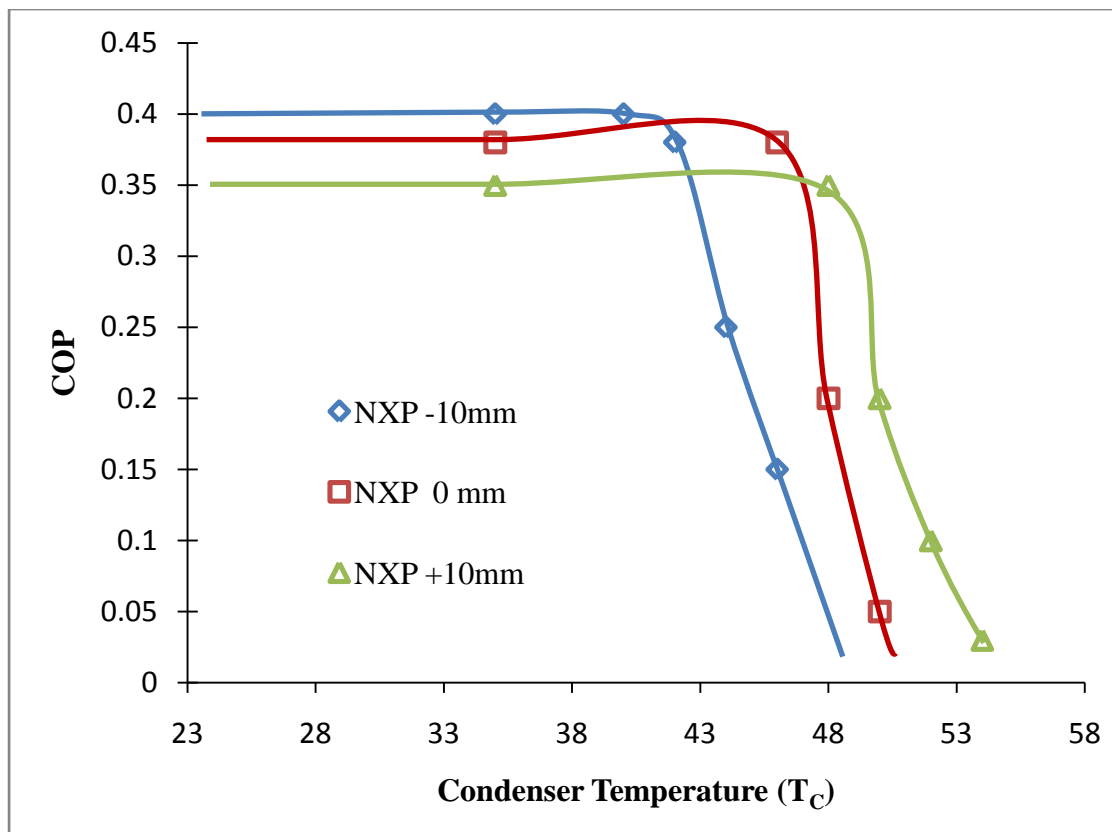
Figure 2.7: Effect of Nozzle position on system COP for different Condenser Temperatures. ($T_g = 130^oC$, $T_e = 5^oC$)

However it should also be noted that for a negative nozzle position, while the COP increases slightly, the critical condenser temperature after which the COP drops

rapidly is the lowest. So the benefit of higher COP is offset by lower critical

temperature.

The size of the nozzle also affects the performance. Varga et al [23] compared nozzle

efficiencies with condenser temperatures for different nozzle sizes and found that the

efficiencies remains more or less constant despite changing the condenser

temperatures if the nozzle diameter is maintained constant. However different

efficiency values are obtained for different nozzle throat diameter values with bigger

nozzles giving greater efficiencies. The variation of nozzle efficiencies with

condenser temperatures is shown in the figure below. The fluid used in the test was

steam. The reader is referred to the parent literature for more details on the design of

the model used.
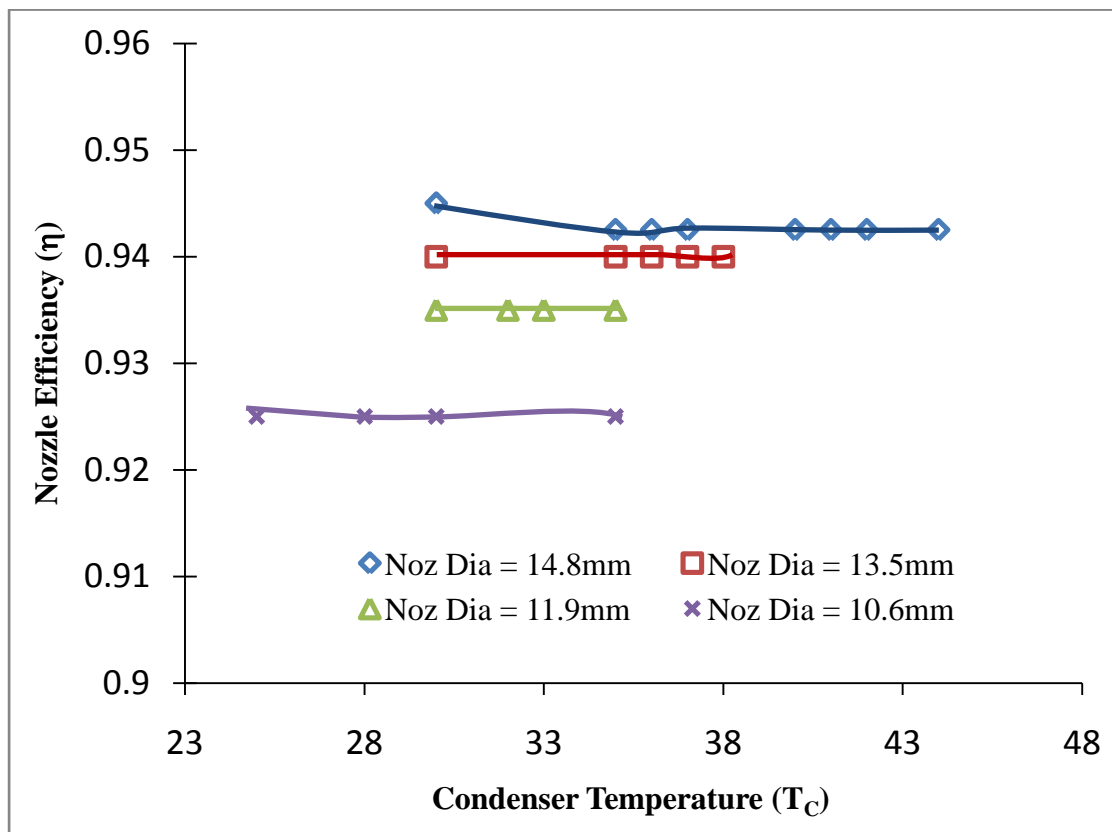
Figure 2.8: Nozzle Efficiencies for different Condenser Temperatures and Nozzle Diameters. ($T_g = 90^oC$, $T_e = 10^oC$)

Other important aspects of nozzle design which affect the performance include converging and diverging cone angles, theoretical area ratios (nozzle outlet area to the throat area) as well as the theoretical nozzle lengths. However, optimum values for these parameters are well documented by ASHRAE [24] in the "Equipments Volume" of the ASHRAE Handbook and are therefore not explained here.

2.2.2   MIXING SECTION

This is the area where the primary and secondary fluids mix together. The primary exiting the nozzle has high velocities and low pressures. By virtue of its low pressure it entrains the secondary fluid and both fluids then mix in the mixing section. The mixing takes place in two stages – Constant Pressure and Constant Area mixing. The first is the constant pressure mixing where the fluids mix at a constant pressure at the cost of their velocities. The pressure remains the same but the primary fluid loses some of its velocity while the secondary gains. At the exit of this section, the fluids are completely mixed having the same pressure and velocity.

The second type of mixing occurs at a constant area. The area remains the same but the mixed fluid decelerates as it flows along the length. When the velocities drop to subsonic conditions, shocks occur.

The diameter of the mixing section is an important parameter which affects the performance of the ejector. Normally the ratio of the Mixing section area to the nozzle throat area is studied. The effect of varying the area-ratio on the entrainment was analysed by Ouzzane and Aidoun [25].

R142B was used as a refrigerant and the system was built for a maximum

refrigeration capacity of 5 KW. The Generator Pressure was held at 1000 KPa and the

Evaporator Pressure at 150 KPa. The convergence and divergence angles were

maintained at 5 degrees. The results obtained are shown in Figure 2.9.
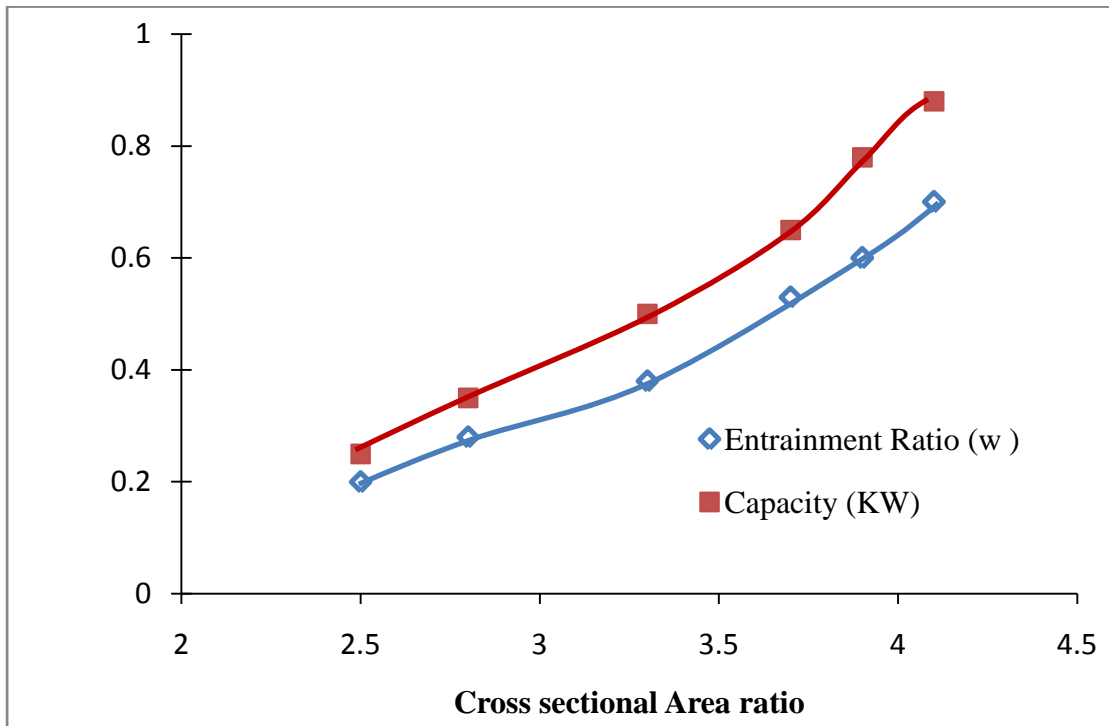
Figure 2.9: Variation of Capacity and Entrainment with Cross sectional Area ratio
(P_g = 1000 KPa, P_e = 150 KPa)

It can be seen that as the area ratio of the ejector is increased, the possible entrainment

increases. As a result, the cooling capacity of the system also increases. However, it

should be noted that a similar condition will result in a decrease in the exit condenser

pressure. So a balance between the entrainment and the exit pressure should be agreed

upon.

2.2.3 DIFFUSER

The diffuser is a diverging section. The flow entering the diffuser is subsonic as a

result of shocks in the mixing section. As the fluid flows along the diffuser, the fluid

decelerates while the pressure increases. At the diffuser exit, the stagnation conditions are achieved. The dimensions of the diffuser depend on the pressure rise required. The equations used to calculate these dimensions are the governing equations for nozzle flow discussed in the previous sections. Normally the effect of diffuser on the ejector performance is considered minimal and is often ignored in design and analysis. A diffuser angle of 3-6 % is normally maintained.

Figure 2.10 shows the usual pressure distribution inside the diffuser as shown by Chunnanond and Aphornratana [22] for a steam ejector with Generator and Evaporator temperatures at $130^{\circ}C$ and $10^{\circ}C$ respectively.
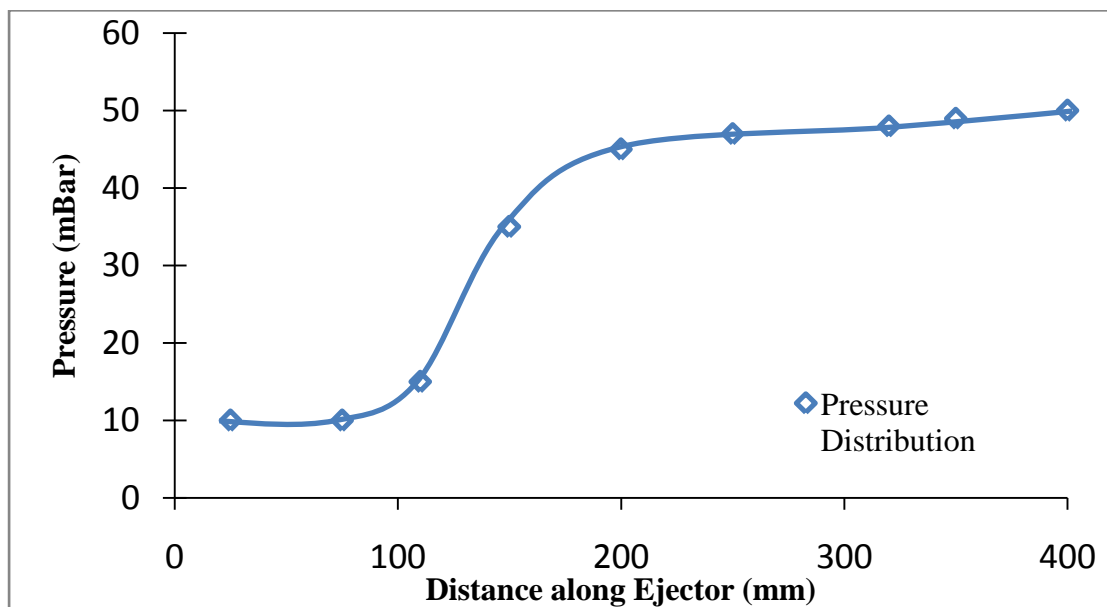
Figure 2.10: Variation of Pressure along the Diffuser of an Ejector
($T_g = 130^{\circ}C$, $T_e = 10^{\circ}C$)

2.3 DRAWBACKS OF A TRADITIONAL EJECTOR SYSTEM

Lack of flexibility and a low attainable thermal COP remain the major drawbacks preventing the widespread usage of Ejector driven systems.

The ejector does not have any mechanically moving component and is thus easy to design, inexpensive to manufacture and easy to maintain. However, this also means that it has a fixed range of operation and cannot be adjusted mechanically or otherwise to suit different operating scenarios.

The traditional ejector driven systems also have a very low thermal COP (or operating efficiency) when compared with a compressor driven refrigeration system. This is a systemic limitation brought about by the ejector as a component itself and no amount of tweaking the operating or geometric parameters will bring a substantial increase.

2.4   MODIFICATIONS TO THE BASIC SYSTEM

The basic ejector system cycle is often modified to improve the performance and enable it's usage in situations where substantial waste heat is not available. One such modified cycle used by Sarkar [26] is shown below
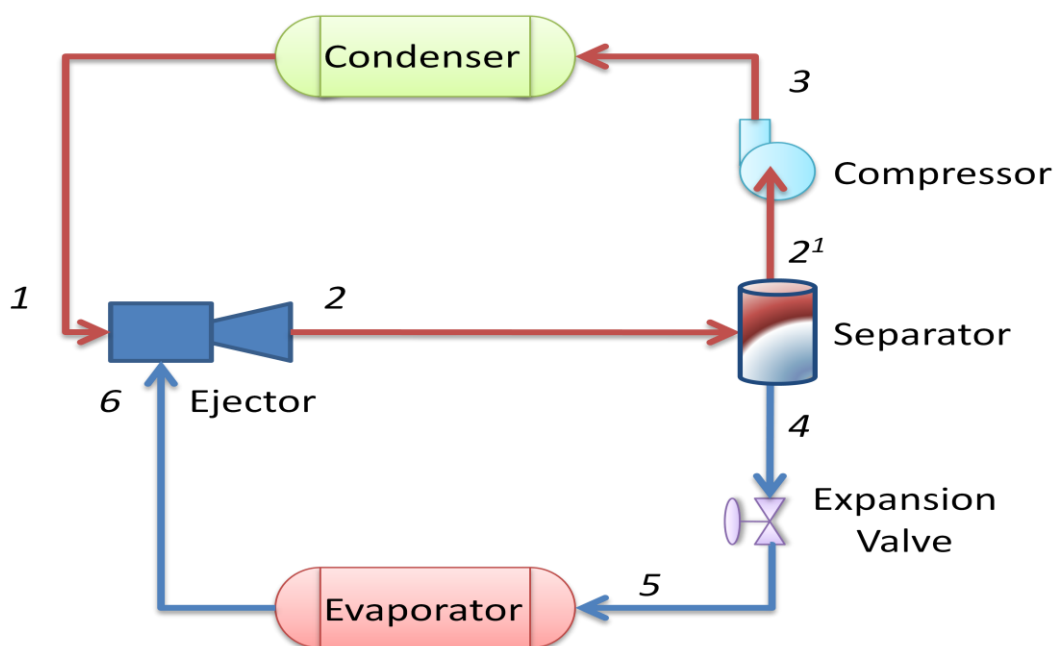
Figure 2.11: Ejector System handling two-phase flow

The Ejector used is a "Two Phase Ejector". The condensed primary fluid is in the liquid phase. The evaporated secondary fluid is in the vapour phase. The pump in the traditional cycle is replaced with a compressor.

Figure 2.12 shows the P-h diagram for such a cycle.
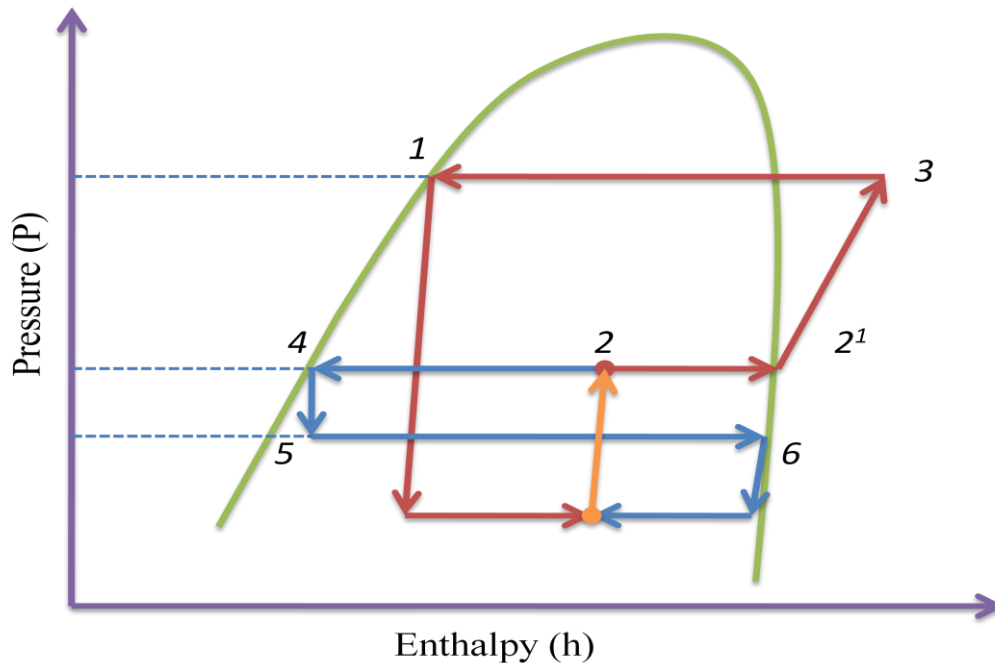
Figure 2.12: P-h diagram for a two-phase ejector

The area to be cooled is the Evaporator (5-6). The heat added to the refrigerant in the Evaporator is rejected in the Condenser (3-1).

The ejector operates in series with and reduces the load on the compressor (2^1-3). The required pressure rise in the system (P_1 minus P_6) is brought about in two stages. The first involves the ejector. It increases the pressure from P_6 to P_2. The compressor takes in fluid from the outlet of the ejector and brings about the remaining pressure rise (P_2 to P_1). When the system is operating in the 'off-peak' condition and the cooling load

on the system is much lesser than the maximum, the ejector is capable of handling the entire load by itself.

Some of the applications for which this cycle is best suited are those of refrigeration and comfort air conditioning. The major advantage remains the non requirement of waste heat to act as a driver. Also the system can be operated using the basic vapour compression refrigeration cycle even if the ejector is removed or taken offline.

2.5   THE ROTODYNAMIC EJECTOR CONCEPT

It was specified earlier that the issue of low COP in traditional ejectors is inherent in the component itself. This is because ejectors in their traditional form depend on "turbulent mixing" of primary and secondary fluids to decelerate and shock the fluids. The pressure increase then occurs along the diffuser. Turbulent mixing is a dissipative process and so, a lot of energy available in the fluid is lost resulting in very low efficiencies.

In Rotodynamic Ejectors, by introducing a rotor-blade arrangement inside the ejector, the energy which is normally lost due to dissipation in the traditional model can be used instead to drive a rotor and increase the discharge pressure. This will improve the efficiency of operation and generate useful power resulting in improved COP.

Explaining this concept as "Pressure exchange", wherein "a body of fluid is compressed by pressure forces that are exerted on it by another body of fluid that is expanding", JV Foa, in his patent application US 3046732 [27] described among other

embodiments, a hollow conical body with circumferential holes canted at an angle. As primary fluid leaves this conical body circumferentially at an angle, it entrains the secondary fluid and exchanges momentum, increasing the pressure of the secondary. If the conical body is supported on bearings, it will be self rotating since the nozzles are canted at an angle. It then behaves like a rotodynamic compressor driven by a turbine and hence we call this development a "Rotodynamic Ejector".

Though developing a similar model would involve among other problems, intricate geometries and severe thrust factoring, the concept is worth exploring in developing a much more efficient ejector.

CHAPTER III

TRADITIONAL EJECTOR MODEL DEVELOPMENT

3.1   INTRODUCTION

This section focuses on the 1D model developed to predict the performance of traditional ejectors. The model displays the possible entrainment and the optimum area ratio of the ejector if the refrigerant, inlet-outlet conditions and the primary nozzle throat diameter are specified. The model can also be scaled to predict the system Mechanical and Thermal Coefficients of Performance (COP).

The governing equations and the assumptions involved are first specified. The calculation scheme followed for analysis is then discussed. Finally the model performance is evaluated by comparing with available experimental data of Huang et al. [18] , Yapici et al. [28] , Hsu [29], Pianthong et al [6] and Selvaraju and Mani [30].

The computer program is written in MATLAB. The thermodynamic properties of fluids are calculated using REFPROP.

3.2   SYSTEM ANALYSIS

3.2.1   ASSUMPTIONS

The following assumptions are made

1. The flow is one dimensional

2. Stagnation conditions prevail at the inlet and exit of the ejector.

3. Primary and Secondary flows are choked at the entry to the mixing chamber.

4. Except for the shocks which occur in the mixing section, the flow is isentropic.

The conventions used in the analysis can be seen in Figure 3.1
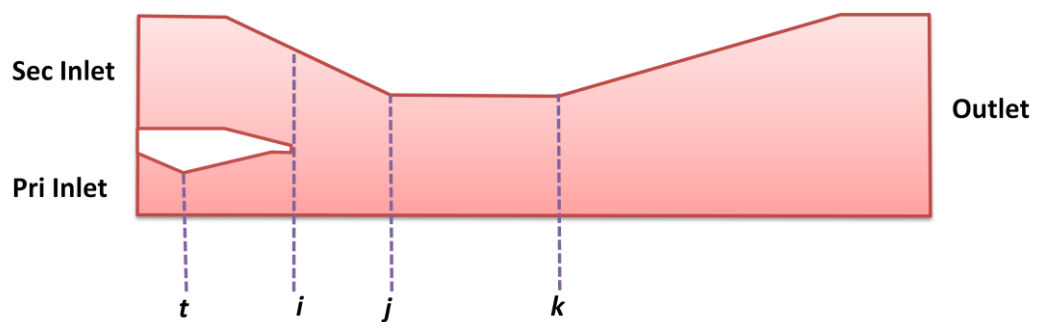
Figure 3.1 Conventions used in 1D Ejector analysis

3.2.2 GOVERNING EQUATIONS

The governing equations are those applicable for 1D compressible flow and the ideal gas law. For an arbitrary variable area volume shown in Figure 3.2,
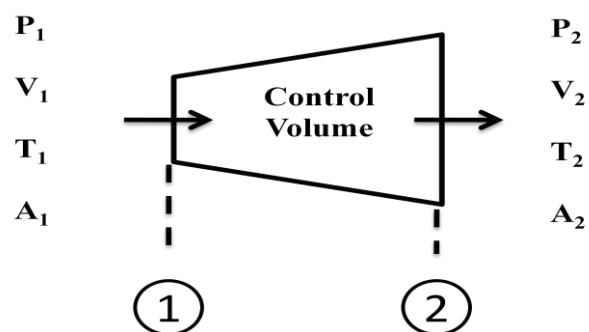
Figure 3.2 Control Volume for 1D flow

Continuity Equation

$$\rho_1 \, A_1 \, V_1 \; = \; \rho_2 \, A_2 \, V_2 \tag{3.1}$$

Momentum Equation

$$P_1 \, A_1 + m_1 \, V_1 + \int_{A_1}^{A_2} P \, dA = P_2 \, A_2 + m_2 \, V_2 \tag{3.2}$$

Energy Equation

$$h_1 + \frac{V_1{}^2}{2} = h_2 + \frac{V_2{}^2}{2} \tag{3.3}$$

Ideal Gas Law

$$P = \rho \, R \, T \tag{3.4}$$

Isentropic flow equation

$$\frac{P}{\rho^\gamma} = constant \tag{3.5}$$

Mach Number

$$M = \frac{V}{\sqrt{\gamma \, R \, T}} \tag{3.6}$$

These basic equations can be related to their respective stagnation states by the following equations

$$\frac{P}{P_0} = \left[1 + \left[\frac{\gamma - 1}{2}\right] M^2\right]^{-\left(\frac{\gamma}{\gamma-1}\right)} \tag{3.7}$$

$$\frac{T}{T_0} = \left[1 + \left[\frac{\gamma - 1}{2}\right] M^2\right]^{-1} \tag{3.8}$$

$$\frac{\rho}{\rho_0} = \left[1 + \left[\frac{\gamma - 1}{2}\right] M^2\right]^{-\left(\frac{1}{\gamma-1}\right)} \tag{3.9}$$

3.2.3   COMPUTATIONAL METHODOLOGY

The computational method followed by the 1D model is explained in detail in this section. The equations used are all derived from the governing equations mentioned in the previous section. Thermodynamic properties at individual states are found by interfacing the computational code with REFPROP.

The inlet and outlet conditions of the Ejector are specified as Primary Inlet Pressure (P_{pri}) and Temperature (T_{pri}), Secondary Inlet Pressure (P_{sec}) and Temperature (T_{sec}) and Outlet Pressure (P_{out}) and Temperature (T_{out}).

The Nozzle throat diameter (D_t) is then specified.

The enthalpies at the inlets and outlet can then be calculated.

$$h_{pri} = f\left(T_{pri}, P_{pri}\right) \tag{3.10}$$

$$h_{sec} = f\left(T_{sec}, P_{sec}\right) \tag{3.11}$$

$$h_{out} = f\left(T_{out}, P_{out}\right) \tag{3.12}$$

The Mach number of the secondary fluid at section 'i' can be calculated as

$$M_{sec-i} = \sqrt{\frac{2}{\gamma - 1}\left[\left(\frac{P_{sec}}{P_i}\right)^{\frac{\gamma-1}{\gamma}} - 1\right]} \tag{3.13}$$

Since we assume the flow to be choked, $M_{sec-i} = 1$. We can then find P_i

The Mach number of the primary fluid at the exit of the nozzle is then

$$M_{pri-i} = \sqrt{\frac{2}{\gamma - 1}\left[\left(\frac{P_{pri}}{P_i}\right)^{\frac{\gamma-1}{\gamma}} - 1\right]} \tag{3.14}$$

At the constant pressure mixing section, the conservation equations can be written as

Mass conservation:
$$m_{pri-i} + m_{sec-i} = m_j \tag{3.15}$$

Momentum conservation:
$$m_{pri-i}\left(V_{pri-i}\right) + m_{sec-i}\left(V_{sec-i}\right) = m_j\left(V_j\right) \tag{3.16}$$

Energy conservation:
$$m_{pri-i}\left(h_{pri-i}\right) + m_{sec-i}\left(h_{sec-i}\right) = m_j\left(h_j\right) \tag{3.17}$$

Sun and Eames [2] combined these equations to give

$$M_j^* = \frac{M_{pri-i}^* + \omega M_{sec-i}^*\sqrt{\frac{T_{sec}}{T_{pri}}}}{\sqrt{\left(1 + \omega\frac{T_{sec}}{T_{pri}}\right)(1 + \omega)}} \tag{3.18}$$

The relationship between M and M^* is given by

$$M = \sqrt{\frac{2M_*^2}{\gamma + 1 - M_*^2(\gamma - 1)}} \tag{3.19}$$

At the constant area section, the mixed fluid experiences a shock which causes a

pressure rise while reducing the velocity to subsonic condition.

The Mach No of the mixed fluid after the shock at section 'k' is given by

$$M_k = \sqrt{\frac{2 + (\gamma - 1)M_j^2}{1 + 2\gamma M_j^2 - \gamma}} \qquad (3.20)$$

Then the Pressure at section 'k' can be found by

$$P_k = \frac{P_{out}}{\left[1 + \left(\frac{\gamma - 1}{2}\right) M_k^2\right]^{\frac{\gamma}{\gamma - 1}}} \qquad (3.21)$$

P_k can be related to the area ratio $\left[\frac{A_t}{A_k}\right]$ and the entrainment ratio [ω] using the following expression by Sun and Eames [2] ;

$$\frac{A_t}{A_k} = \frac{\frac{P_{out}}{P_{pri}}}{\sqrt{(1 + \omega)\left(1 + \omega\frac{T_{sec}}{T_{pri}}\right)}} \frac{\left(\frac{P_k}{P_{out}}\right)^{\frac{1}{\gamma}}\sqrt{1 - \left(\frac{P_k}{P_{out}}\right)^{\frac{\gamma - 1}{\gamma}}}}{\left(\frac{2}{\gamma - 1}\right)^{\frac{1}{\gamma - 1}}\sqrt{1 - \frac{2}{(\gamma - 1)}}} \qquad (3.22)$$

The entrainment ratio [ω] and the Area ratio $\left[\frac{A_t}{A_k}\right]$ can be found by simultaneously solving these equations.

If the schematic of the system under investigation is known, the Coefficient of Performance (COP) can be calculated.

COP is defined as the ratio of the refrigeration effect obtained to the work input given to the system. Sun [31] noted that two conventions of COP are commonly used; Thermal and Mechanical COP.

The Thermal Coefficient of Performance of the cycle is defined as the ratio of Refrigeration Effect to the Thermal Work Input to the system. It can be calculated by the following formula in equation (3.23)

$$COP_{thermal} = \frac{Q_e}{Q_g + W_p} \tag{3.23}$$

Neglecting the work done on the pump ($W_p = 0$),

$$COP_{thermal} = \omega \left[\frac{\Delta h_e}{\Delta h_g} \right] \tag{3.24}$$

The Mechanical Coefficient of Performance is concerned only with the mechanical work input into the system. So it can be defined as in equation (3.25) and (3.26)

$$COP_{mech} = \frac{Q_e}{W_p} \tag{3.25}$$

$$= \omega \left[\frac{\Delta h_e}{\Delta h_p} \right] \tag{3.26}$$

The overall sequence followed for computation can be understood from Figure 3.3
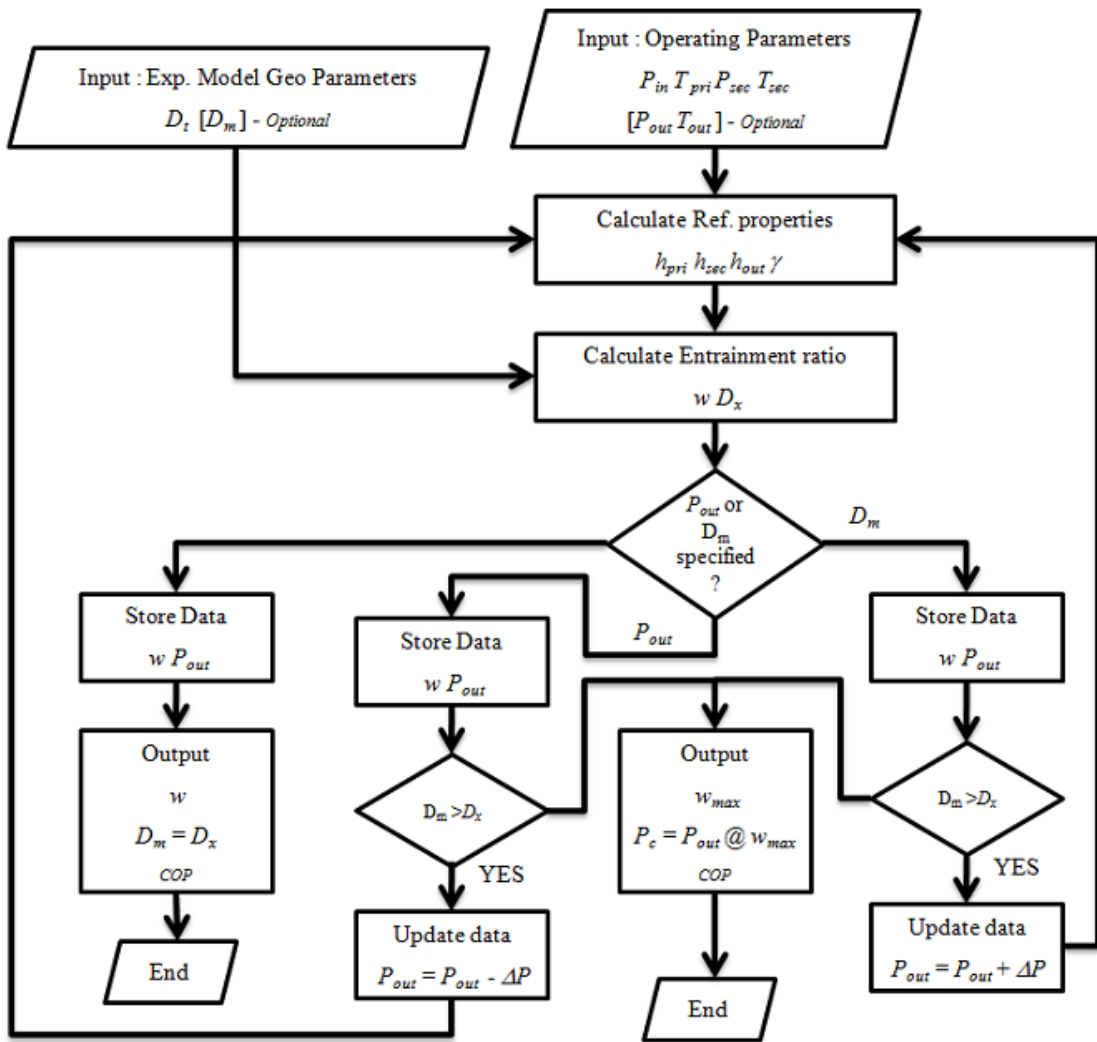
Figure 3.3 Computational Sequence of the 1D model

CHAPTER IV

RESULTS AND DISCUSSION

4.1   INTRODUCTION

This Chapter is divided into two parts. The first part deals with "Model Validation". The 1D model developed in Chapter III is validated with experimental data available in the literature. Validation is essential to ensure the model is acceptable and can be used to support decision making. The ultimate goal of model validation is therefore to make the model useful in the sense it addresses the right problem and provides accurate information about the system being modelled. Section 4.2 deals with this aspect.

Once a model is validated, it can be used to make predictions. This is the subject of the second part of this chapter. The validated model is used for alternate refrigerant predictions. The systems for which alternate refrigerants are predicted are those that are already in existence and were used by researchers to carry out prior studies. Sections 4.3 through 4.5 address these aspects.

4.2   MODEL VALIDATION

The developed 1D model has been "data validated" by comparing it's output data, given similar input data, with that of many other experimental models available in literature. The physicals models used as the standard were those experimented by Huang et al. [18], Hsu [29], Pianthong et al [6] and Selvaraju and Mani [30] . The

output parameters compared were the entrainment ratio and COP. The inputs were the model geometric parameters and operating conditions. The results are shown graphically as Figures 4.1 and 4.2.
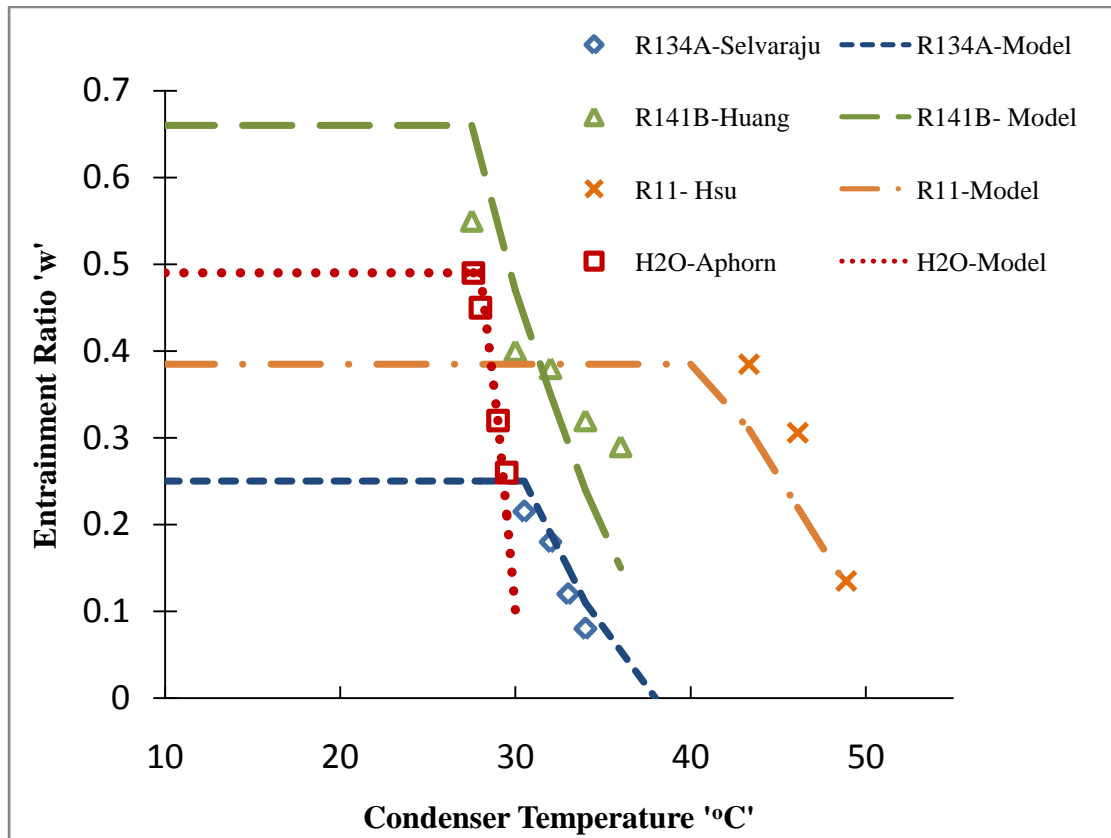
Figure 4.1: Model Validation – Entrainment ratio prediction

Figure 4.1 shows the variation of entrainment ratios with changes in condenser temperatures. The dotted lines show the values predicted by our 1D model. The symbols represent the corresponding experimental values obtained by the researchers. It can be seen that the model predictions are in close agreement with the available experimental results. In addition to the entrainment ratio variation, our model is also able to predict the critical condenser temperature accurately.

Figure 4.2 shows the comparison of the COP predicted by the 1D model and the experimental results obtained by Yapici et al. [28].
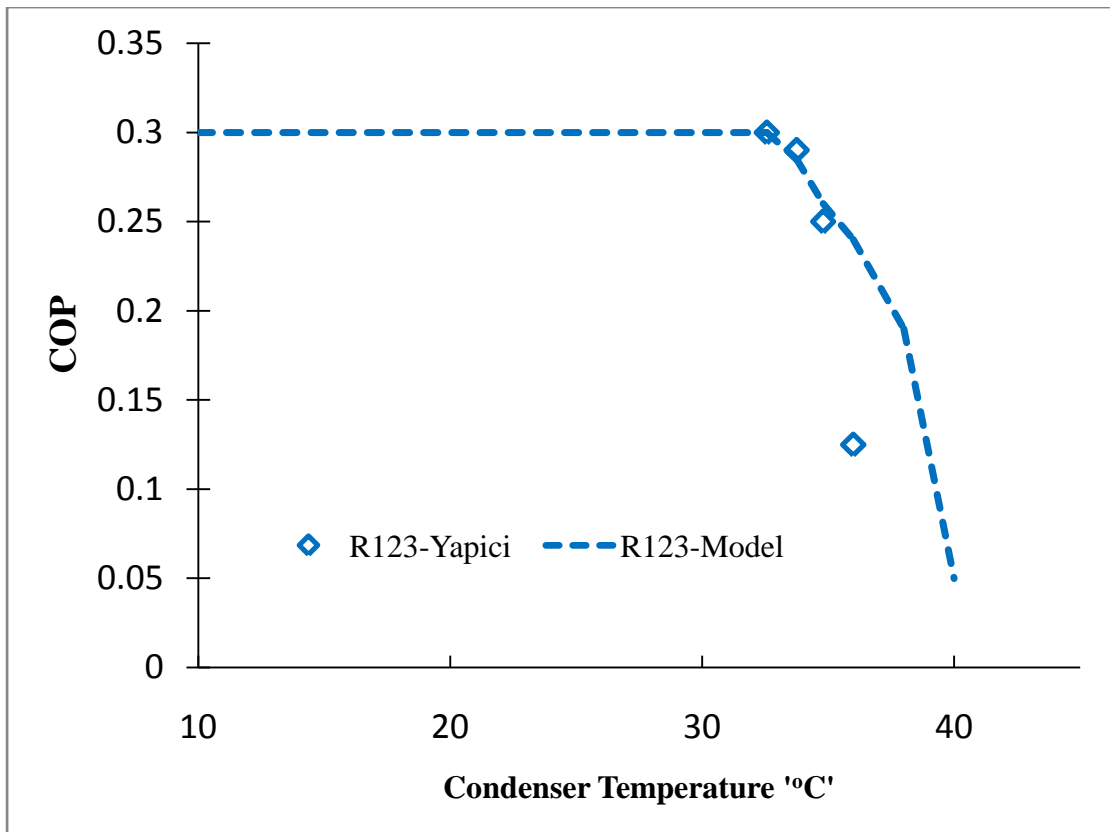
Figure 4.2: Model Validation – COP prediction

The COP used for comparison is the thermal COP. Once again the model's predicted values do not deviate much from the values obtained by experiments.

We therefore conclude that our model is validated to predict the real world ejector performance conditions. We can now use it to determine performance of refrigerants for which no physical models are available and make qualitative and quantitative predictions.

4.3   BACKGROUND FOR ALTERNATE REFRIGERENT PREDICTION

A refrigerant is a substance used in a heat cycle for enhanced efficiency. It usually involves reversible phase change from a liquid to a gas. The ideal refrigerant has

favourable thermodynamic properties, is non-reactive chemically, and safe. The desired thermodynamic properties are a boiling point somewhat below the target temperature, a high heat of vaporization, a moderate density in liquid form, a relatively high density in gaseous form, and a high critical temperature. Since boiling point and gas density are affected by pressure, refrigerants may be made more suitable for a particular application by choice of operating pressure. Corrosion properties are a matter of materials compatibility with the mechanical components: compressor, piping, evaporator and condenser. Safety considerations include toxicity and flammability [32].

These properties are ideally met by Chloro Flouro Carbons (CFC) like CFC11, CFC12, CFC113 etc. and therefore in the late 1980s and early 1990s most of the ejector-oriented research was focussed on using these fluids as refrigerants (Tyagi and Murty [33], Chen and Hsu [34], Nahdi et al. [35]). Another reason for considering these refrigerants, especially CFC11 was its low boiling point at atmospheric pressure. This enabled easy design and maintenance of ejector systems. However CFCs have a very high Ozone Depletion Potential (ODP). So production and usage of CFC11 and other CFCs was subsequently banned by the Montreal Protocol. The different refrigerants and their ODP are shown in Figure 4.3

The Ozone Depletion Potential (ODP) of a refrigerant is calculated in relation to R11. Manzer [36] defined it as the ratio of cumulative calculated ozone depletion caused by the release of a compound / refrigerant to the calculated ozone depletion caused by an equal emission (by weight) of R11. In a similar manner, the relative halocarbon Global Warming Potential (halocarbon GWP) is also calculated.
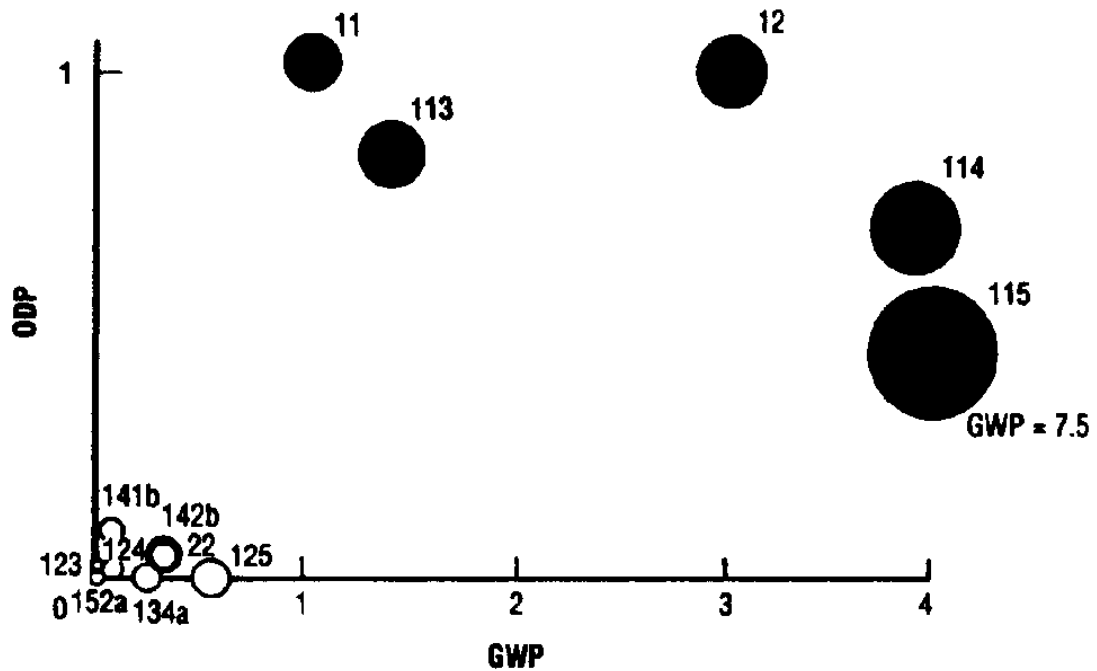
Figure 4.3: Relative ODP and Halocarbon GWP of different CFCs, HCFCs and HFCs

The Figure 4.3 shows the calculated ODP and GWP values of different refrigerants relative to R11 which is assigned a value of 1. The area of each circle is proportional to the atmospheric lifetime of the refrigerant. Solid circles represent CFCs which are halogenated. Hollow circles represent HCFCs and HFCs.

It can be seen that most CFCs have a high ODP and GWP. Also their lifetimes in the atmosphere are very large when compared to HCFCs and HFCs. Therefore they were the first ones to be banned in the effort to repair the ozone layer and neutralise global warming.

4.4   OZONE LAYER DEPLETION

4.4.1   OUTLINE OF THE PROBLEM

The Ozone layer in the stratosphere of the earth's atmosphere is a protective layer which filters the sun's harmful ultraviolet radiations from reaching the earth. In recent years, it has been noticed that the protective layer is getting destroyed by manmade chemicals like CFCs, halons etc. The primary usage of these chemicals is in refrigeration, air conditioning and fire extinguishing systems.

These substances, when emitted, are so stable that they will reach the stratosphere, where they are decomposed by strong solar ultraviolet rays, releasing atoms of chloride or bromine. With those atoms serving as catalysts, the reaction in which ozone is decomposed takes place in a chain reaction. Once the ozone layer is depleted by CFCs, it will take much time for it to restore causing widespread damage around the world. In addition to causing health disorders, such as nom-melanoma skin cancer and cataracts in humans, it would also hamper the growth of plants and planktons.

4.4.2   OZONE LAYER PROTECTION MEASURES

In order to prevent the depletion of ozone layer, CFCs and halons were termed as controlled substances and in November 1992, the parties to the Montreal Protocol brought out the phase out schedule for controlled substances. Table 4.1 shows the controlled substances and their phase out schedules.

Table 4.1 - Phase-out Schedule adopted by the fourth Meeting of the Parties to the Montreal

Protocol (November 1992)

Substance	Phase- out Schedule
CFC-11, 12, 113, 114, 115	Freeze at 1986 level by 1989
	75% reduction of 1986 level by 1994
	Total phase out by 1996
Halon-1211, 1301, 2402	Freeze at 1986 level by 1992
	Total phase out by 1994
	20% reduction of 1989 level by 1993
CFC-13, 111, 112, 211, 212, 213, 214, 215, 216, 217	75% reduction of 1989 level by 1994
	Total phase out by 1996
Carbon tetrachloride	85% reduction of 1989 level by 1995
	Total phase out by 1996
1, 1, 1-trichloroethane (methyl chloroform)	Freeze at 1989 level by 1993
	50% reduction of 1989 level by 1994
	Total phase out by 1996
HCFC*	Freeze at the standard level by 1996
	35% reduction of the standard level by 2004
	65% reduction of the standard level by 2010
	90% reduction of the standard level by 2015
	99.5% reduction of the standard level by 2020
	Total phase out by 2030
HBFC	Total phase out by 1996
Methyl bromide	Freeze at 1991 level by 1995
	(except the amounts used for quarantine and pre-shipment applications)

* The standard level = 1989 caluculated consumption level of HCFC
+1989 caluculated consumption level of CFC×0.031

This schedule emphasised on total phase out of R11 and other CFCs, halons and carbon tetra chloride by 1996.

The HCFCs, which are next in line, their production is to be frozen at the standard level by 1996 and they are to be phased out by 2030.

4.5   REPLACEMENTS FOR R11

With R11 banned by the Montreal protocol, R123 was proposed as the most suitable short-to-medium term replacement for R11 (Sun and Eames [2], Yapici et al. [28]). R141b was also very popular among researchers (Huang and Chang [3]).

However these refrigerants fall under HCFCs and the production of these are also restricted with a total phase out planned by 2030. So the search for newer refrigerants is on once again.

4.6   NEED FOR REFRIGERANT EVALUATION MODELS

While determining a replacement, it is essential to consider how the prospective replacement will perform in service and under similar operating conditions. Physical testing to evaluate the performance of every possible replacement is costly, tedious and time consuming. An alternate cost effective way would be to develop computer models which can mimic the expected performance of each replacement and the base refrigerant in the system.

The model could then be used to determine the expected performance of any prospective replacement refrigerant. This would be faster while giving us just as good a picture. It would also enable us to test an unlimited range of refrigerants and blends to select the optimum fluid for our operation. This is precisely the purpose of this section.

4.7 EVALUATION STRATEGY ADOPTED

Physical ejector models, developed by researchers and using refrigerants which are now banned / restricted are considered. The banned / restricted refrigerant is termed as the base refrigerant for each physical model. The performance of each physical model with the base refrigerant is modelled with the 1D model discussed in the previous section to validate the model. Then the refrigerant is replaced with a target environment friendly refrigerant and the expected performance is determined. This process is repeated for a range of environment friendly refrigerants. The results are used to determine the best alternate refrigerant.

Base refrigerants considered are R11, R123 and R141b. The replacement refrigerants modelled are R134a, R245fa, R245ca, Ammonia and Water / Steam.

4.8 BASE REFRIGERANT - R11

4.8.1 THE MODEL

The experimental model used is that of Hsu [29]. The Generator's outlet conditions are imposed at the primary fluid inlet of our model. Evaporator's outlet and the Condenser's inlet conditions are used at the secondary inlet and the diffuser outlet respectively. The Diameter at the nozzle throat [D_t] is 0.344m and the Area ratio [AR] is 5.01. Across the refrigerants, the temperatures at the inlets and exits are used as the references.

4.8.2   VARIATION OF ENTRAINMENT RATIO

The entrainment ratio is defined as the ratio of the secondary mass flow entrained to the mass flow of the primary driver. Figure 4.4 shows the variation of entrainment ratio with increase in the condenser temperature for R11 and all the alternate refrigerants tested. Water was found to be unsuitable for use as the area ratio required for optimum operation is much larger.

It is noticed, for the same generator and evaporator conditions, as the condenser temperature is increased, the entrainment ratio remains constant till a critical point. Further increase in the condenser temperature results in a rapid drop in entrainment.
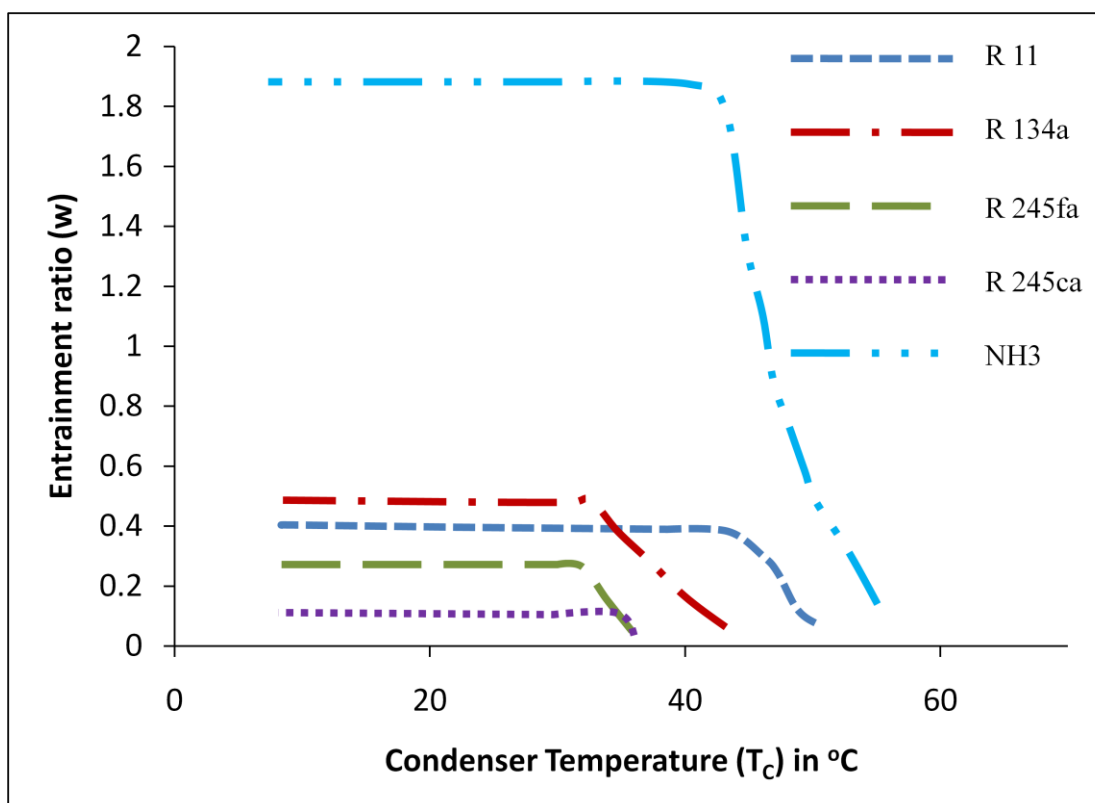
Figure 4.4: R11 and Replacements Entrainment ratios attainable at $T_G = 93.3$ ^{o}C, $T_E = 10$ ^{o}C, $D_t = 0.344$m, $D_m= 0.77$m

As the condenser temperature is increased, the shocks in the constant area mixing section move towards the primary nozzle. When the condenser temperature is increased beyond the critical point, the shocks are no longer in the constant area section. They have already moved close to the primary nozzle and the entrained secondary fluid no longer reaches sonic conditions. Therefore at higher condenser temperatures, the entrainment ratio drops rapidly.

Among the refrigerants tested, Ammonia gives the highest entrainment ratio of 1.8, ie the mass flow rate of the entrained secondary fluid of the ejector is 1.8 times the mass flow rate of the primary fluid. Ammonia is followed by R 134a with an entrainment of 0.48. Both these fluids give a higher entrainment than can be attained by using R11. So if R11 is replaced with Ammonia or R134a, more secondary fluid will be entrained by the ejector for a given primary fluid mass flow rate resulting in greater heat removal capacity of the evaporator. The entrainment ratios obtained by R 245fa and R245ca are lesser than the base refrigerant and are therefore not suitable replacements from the entrainment point of view.

4.8.3   CHANGE IN CRITICAL PRESSURE AND TEMPERATURE

It was mentioned in the previous section that as the condenser temperature increases, the entrainment remains constant up to a certain value and then drops rapidly. The highest condenser temperature and its corresponding pressure at which the entrainment remains the maximum are the critical points. These points represent the highest condenser temperatures and pressures that can be handled by the ejector while maintaining the entrainment and the 'double choked' condition.

From Figure 4.4, it can be seen that the critical condenser temperature obtained by ammonia (43.33^{o}C) is very close to that of R11. All the other refrigerants have lower values. The critical temperatures for R134a, R245fa and R245ca are 33°C, 30°C and 35°C respectively. The critical pressures are the saturation pressures corresponding to the corresponding critical temperatures.

4.8.4   CHANGE IN PRESSURE LIFT AND COP

The pressure lift (ΔP) is defined as the ratio of the Critical Exit or Condenser Pressure to the Secondary fluid inlet pressure. The pressure lift obtained by using R11 is 3.19. None of the alternate refrigerants match the pressure lift achievable by R11, but R245fa (ΔP = 2.31) and R245ca (ΔP = 2.67) are the closest alternatives. The operating pressures of R245fa (P_c = 1.92bar) and R245ca (P_c = 1.46bar) are also the closet to R11 (P_c = 1.93bar). These variations can be seen in Table 4.1.

The COP considered is the Thermal COP or the System COP. The Base refrigerant R11 develops a COP of 0.223. R134a and Ammonia project an improvement in COP over that obtained by R11. R134a develops a COP of 0.89 and Ammonia develops a COP of 1.47. However, the corresponding values of R245fa and R245ca are much lesser. R245fa develops a COP of 0.1 and R245ca develops 0.05.

4.8.5   REPLACEMENT SUGGESTIONS

The selection of an alternative refrigerant should be made only after considering all the requirements of the application and the implications of the change.

If entrainment is the primary area of concern, ammonia is the best choice. For the same temperature range, it develops a much higher entrainment, but the associated operating pressures to be encountered are much higher ($P_c = 1.93$bar for R11 vs $P_c = 6.93$bar for ammonia). Also the operating margin will be much lesser at higher temperatures because of the bell-shaped P-h curve of Ammonia.

R245fa and R245ca have operating pressure ranges similar to R11 as discussed in section 4.8.4 and will be optimum for use as thermal compressors, but using them will compromise the entrainment. So these refrigerants are choices when the entrainment is not as important as the system pressure.

R 134a is the median choice. It provides a marginally higher entrainment (0.39 for R11 vs 0.48 for R 134a) and improved COP (0.223 for R11 vs 0.896 for R134a). However, similar to ammonia, the operating pressures encountered are much higher than that required for R11. So this refrigerant can be considered if the entrainment cannot be compromised and the system has been designed to handle higher operating pressures.

4.9 BASE REFRIGERANT - R 123

4.9.1 THE MODEL

The experimental model used for comparison is that of Yapici [28]. The diameter at

the nozzle throat [D_t] is 3.21mm and the Area ratio [A.R] is 6.56. The performance of

R123 is compared with other new age refrigerants. The results are tabulated in Table

4.1. The variation of critical condenser temperatures and their corresponding

entrainment ratios are also shown graphically in Figure 4.5.
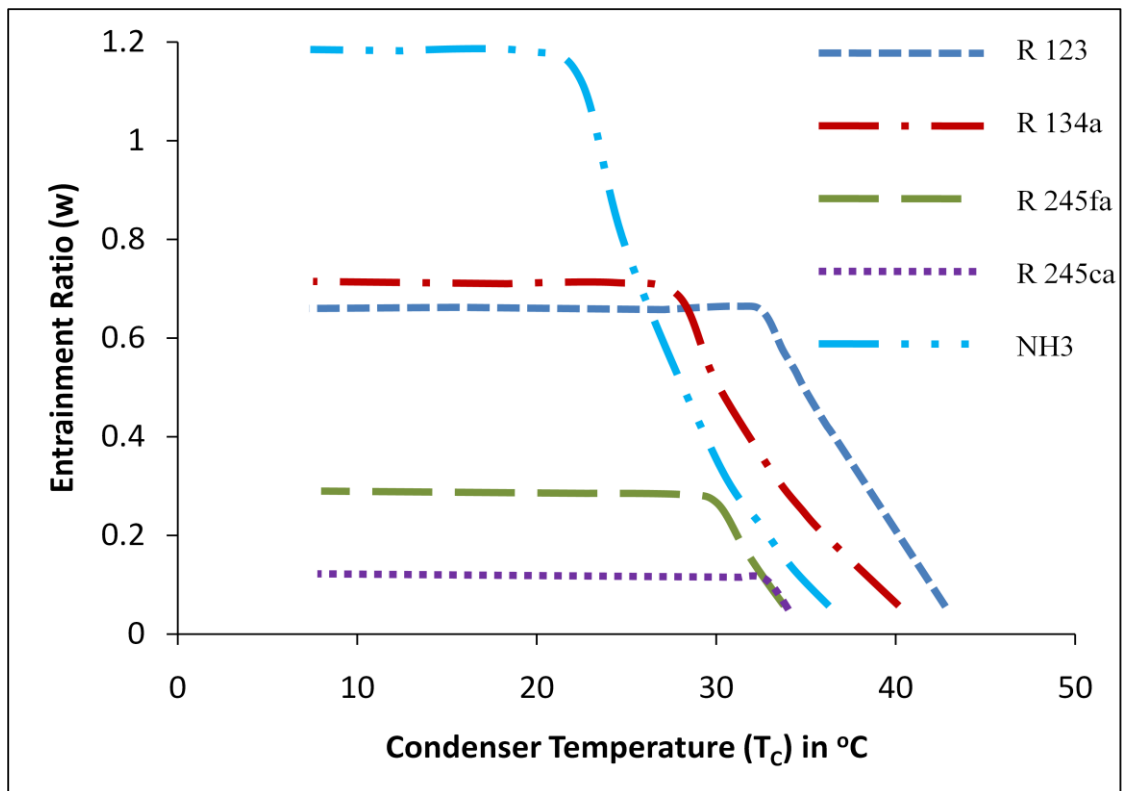
Figure 4.5: R123 and Replacements - Entrainment ratios attainable at T_G = 83 ^{o}C,

T_E = 10 ^{o}C, D_t = 3.21mm, D_m= 8.22mm

4.9.2 VARIATION OF ENTRAINMENT RATIO

The definition for entrainment ratio is given in Section 4.8.2

For the same inlet and geometric conditions, ammonia gives the highest entrainment ratio of 1.12 followed by R134a, R245fa and R245ca. Similar to that of the R11 base model, replacement refrigerants Ammonia and R134a result in higher entrainment than the base refrigerant R123. However the improvement in entrainment is very small in case of R134a (4.6%).

R245fa and R245ca result in much lesser entrainment compared to R123 and are not suitable alternatives from the entrainment point of view. R245fa entrains around 58% lesser than R 123. R245ca fares even worse. It entrains around 81% lesser.

The use of water as a refrigerant was limited in this model due to insufficient area ratio available in the physical model considered. If refrigerant R123 is replaced with water for this physical model, the ejector will malfunction.

4.9.3 CHANGE IN CRITICAL PRESSURE AND TEMPERATURE

The definition of critical pressure and temperature can be read from Section 4.8.3. These are the parameters which define the useful operating range for a given set of inlet conditions. A higher critical pressure and temperature implies a wider useful operating margin and a lower critical pressure and temperature value indicates a smaller or restricted operating margin.

The critical condenser temperature obtained by R245ca is the same as that obtained by the base refrigerant R123 (T_c = 32.57^{o}C). All the other refrigerants have slightly lower values. R245fa has a value of 30°C. R134a and Ammonia have values of 28°C and 22.5^{o}C respectively. The critical pressures are the saturation pressures corresponding to the corresponding critical temperatures.

4.9.4   CHANGE IN PRESSURE LIFT AND COP

The Pressure lift and COP as defined in Section 4.8.4 are an indication of the usefulness of the component as a thermal compressor.

Only R245ca (ΔP = 2.43) matches the pressure lift attained by R123 (ΔP = 2.4). The values achievable by other refrigerants are slightly lesser but still comparable. These details can be read out from Table 4.1. Ammonia provides the least lift of 1.51

R134a projects a 50% improvement in COP over that obtained by R123. Other refrigerants are unable to match the base refrigerant's COP. The worst performer is R245ca which has a COP of only 0.056

4.9.5   REPLACEMENT SUGGESTIONS

If entrainment is the primary area of concern, ammonia is the best choice for replacement. It predicts over 72% improvement in entrainment, but the associated operating pressures are much higher (around 87%). Also the operating margin will be

much lesser at higher temperatures because of the bell-shaped P-h curve. R134a also predicts an entrainment slightly higher than the base refrigerant (around 4.6%). R245fa and R245ca have operating pressure ranges similar to R123, but using them will compromise the entrainment.

If the intention is to replicate the performance of R123 while tolerating higher pressures, R 134a is the optimum choice. It entrains as much as the base refrigerant and also has a stable operating range unlike ammonia.

4.10   BASE REFRIGERANT R141B

4.10.1 THE MODEL

The model used is that of Huang and Chang [3]. The Diameter of the nozzle throat [D_t] is 2.64 mm. The Area ratio [A.R] is 9.44. The results are tabulated in Table 4.1. The variation of critical condenser temperatures and their corresponding entrainment ratios are shown graphically in Figure 4.6. Water could not be tested as entrainment is limited by the area ratio.

The definitions and importance of Entrainment ratio, Critical Pressure and Temperature, Pressure lift and COP can be understood from Sections 4.8.2 to 4.8.4
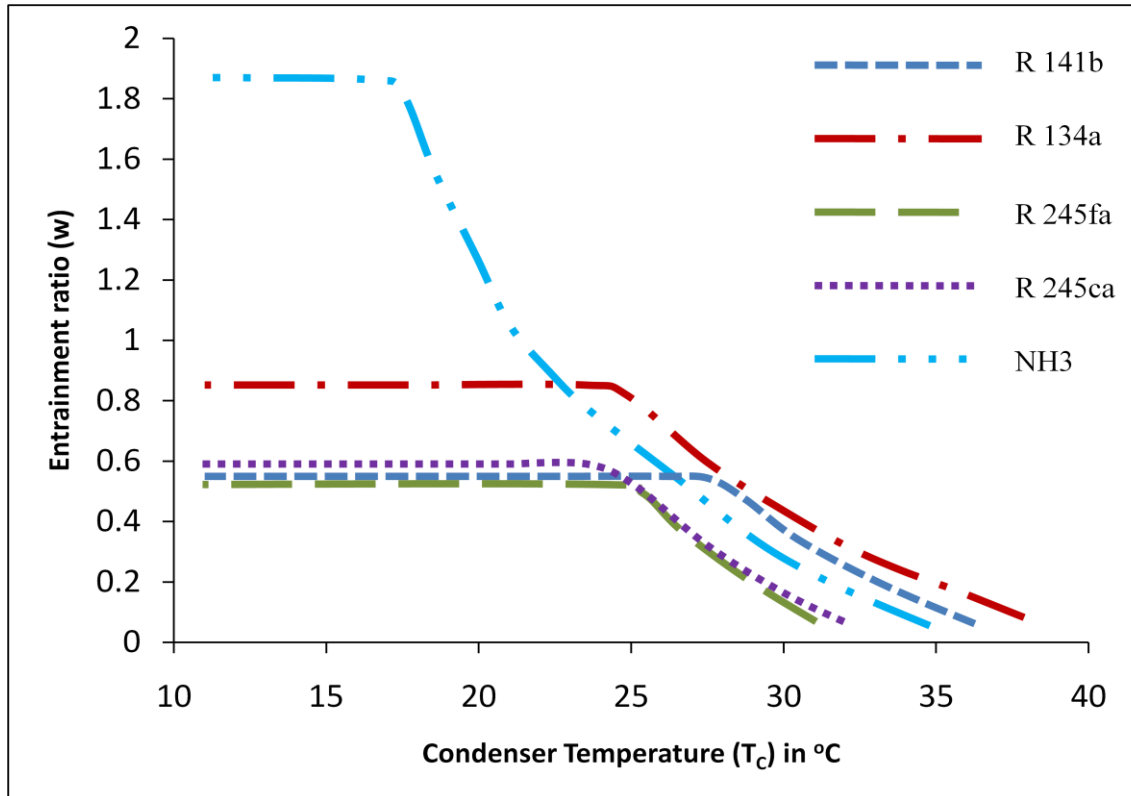
Figure 4.6: R141b and Replacements - Entrainment ratios attainable at T_G = 84 ^{o}C, $T_E = 8 \ ^o$C, D_t = 2.64mm, D_m= 8.11mm

4.10.2 VARIATION OF ENTRAINMENT RATIO

All the alternate refrigerants tested project an entrainment equal to or greater than the base refrigerant. Ammonia ($\omega = 1.82$) and R 134a ($\omega = 0.82$) have a higher entrainment ratio while R 245fa ($\omega = 0.54$) and R245ca ($\omega = 0.58$) entrain as much as R141b ($\omega = 0.55$). So if entrainment is the primary concern, any of the alternates could be used as a replacement

As mentioned in previous sections, a higher entrainment means more secondary fluid is entrained for a given quantum of primary fluid. This indicates that the ejector will operate at high levels of efficiency.

4.10.3 CHANGE IN CRITICAL PRESSURE AND TEMPERATURE

The critical condenser temperatures obtained by R134a, R 245fa and R245ca (T_c = 25°C for all three refrigerants) are closely lumped with that obtained by R141b (T_c = 27.5^{o}C).The values attained by Ammonia are a bit lower (T_c = 17.5^{o}C). The critical pressures are the saturation pressures corresponding to the corresponding critical temperatures.

The critical pressures and temperatures, as mentioned in previous sections, are indicators of the useful range of operation for the component.

4.10.4 CHANGE IN PRESSURE LIFT AND COP

The Pressure lift is an indicator of the aptness for use as a thermal compressor. The Pressure lifts obtained by all the alternate refrigerants are comparable to the base refrigerant. R 245ca (ΔP = 2.02) and R245fa (ΔP = 1.96) are the closest to the base refrigerant (ΔP = 2.15).

COP is an indicator of the cycle efficiency. Ammonia and R 134a display a COP which is greater than the base refrigerant. The base refrigerant has a COP of 0.23. R134a has a COP of 0.476, an improvement of over 100%. Ammonia has a COP of 0.27, an improvement of 17 %.

4.10.5 REPLACEMENT SUGGESTIONS

From the entrainment point of view, all the replacements are suitable alternate refrigerants since they all develop entrainment values equal to or greater than the base refrigerant

From the critical temperature values, R134a, R245fa and R245ca are the best replacement refrigerants.

For maximum COP improvement Ammonia and R134a are the ideal replacements. However their operating pressure values are much higher than the base refrigerant.

4.11 CONCLUSION

The theoretical basis and the computational sequence for the developed model were mentioned in the previous chapter. In this chapter, the prediction results for the performance of a few alternate environment friendly refrigerants were displayed and some suggestions to choose the best replacement were made.

In general, Ammonia seems to be giving the best entrainment performance but it has a very small operating range in addition to higher operating pressures. Therefore when higher pressures in the system can be tolerated, R134a makes a better replacement when compared with ammonia. When lower levels of entrainment can be tolerated and the system hasn't been designed for very high pressures, refrigerants R245fa and R245ca are better replacements.

Table 4.2 Comparison of Performances across Refrigerants

COMPARISON OF PERFORMANCES																							
Base Refrigerant										**Alternate Refrigerant**										**Change** (Alternate - Original)			
	P_G bar	T_G °C	P_E bar	T_E °C	$P_{critical}$ bar	$T_{critical}$ °C	$\Delta P_{critical}$ bar	$w_{critical}$	$COP_{critical}$		P_G bar	T_G °C	P_E bar	T_E °C	$P_{critical}$ bar	$T_{critical}$ °C	$\Delta P_{critical}$ bar	$w_{critical}$	$COP_{critical}$	$P_{critical}$ bar	ΔP bar	w	COP
R11	7.13	93.33	0.61	10.00	1.93	43.33	3.19	0.39	0.223	R134a	34.19		4.15		8.39	33	2.02	0.48	0.896	6.46	-1.17	0.10	0.673
										R245fa	10.85		0.83		1.92	30	2.31	0.27	0.102	-0.01	-0.87	-0.12	-0.121
										R245ca	7.94	93.33	0.55	10	1.46	35	2.67	0.11	0.048	-0.47	-0.52	-0.28	-0.175
										H_2O	0.80		0.01		Entrainment is limited by Area Ratio								
										NH_3	13.21		6.15		6.93	43.33	1.13	1.78	1.469	5.00	-2.06	1.40	1.246
R123	5.27	83	0.50	10.00	1.20	32.57	2.40	0.65	0.290	R134a	28.00		4.15		7.27	28	1.75	0.68	0.447	6.07	-0.65	0.03	0.157
										R245fa	8.49		0.83		1.79	30	2.16	0.27	0.106	0.59	-0.24	-0.38	-0.184
										R245ca	6.15	83	0.55	10	1.34	32.57	2.43	0.12	0.054	0.14	0.03	-0.53	-0.236
										H_2O	0.53		0.01		Entrainment is limited by Area Ratio								
										NH_3	35.00		6.15		9.28	22.5	1.51	1.12	0.231	8.08	-0.89	0.47	-0.059
R141b	4.65	84	0.40	8.00	0.86	27.50	2.15	0.55	0.230	R134a	28.65		3.88		6.65	25	1.72	0.82	0.476	5.79	-0.43	0.27	0.246
										R245fa	8.70		0.76		1.49	25	1.96	0.54	0.162	0.63	-0.19	-0.01	-0.068
										R245ca	6.31	84	0.50	8	1.01	25	2.02	0.53	0.154	0.15	-0.13	-0.02	-0.076
										H_2O	0.56		0.01		Entrainment is limited by Area Ratio								
										NH_3	35.00		5.74		7.91	17.5	1.38	1.82	0.270	7.05	-0.77	1.27	0.040

CHAPTER V

PERFORMANCE ANALYSIS OF ROTODYNAMIC EJECTOR

5.1   INTRODUCTION

An introduction to the concept of Roto-Ejector was given in Chapter II. Turbulent mixing is a dissipative process and the energy, once lost, cannot be recovered. In roto-ejectors, we aim to reduce turbulent dissipation and instead use that energy elsewhere, preferably to do some useful mechanical work. This process is not dissipative and so it is reversible (ie; the useful work can be converted to heat if so desired) and therefore more efficient.

This chapter deals with model development and performance analysis of a Roto-Ejector. The theoretical basics and the dynamics of developing a roto-dynamic ejector are first laid out. The governing equations are then specified and the steps involved in developing a model to predict the performance of a roto-ejector are discussed. The model's performance is then compared with a Traditional Ejector system as well as the existing Vapour Compression Refrigeration system and the improvements are gauged.

It should be noted the model has been developed from an academic stand-point. The intention is only to show that further research in this direction may lead to promising results. Constraints like the intricacy of the geometry, thrust factoring, associated mechanical friction etc have not been considered. A researcher interested in

developing a physical working model would have to allot due weightage to these factors.

5.2   THE TURBO COMPRESSOR ANALOGY

The concept of Roto-Ejector can be better understood by comparing it a Turbine driven compressor (Figure 5.1). The turbine is a mechanical device which is driven by a high pressure fluid. The work done by the fluid on the turbine blades is used to drive a compressor which is directly attached to its shaft. If the process occurring in the turbo machinery is isentropic and thermodynamically reversible, the adiabatic efficiency obtained is optimal [37]
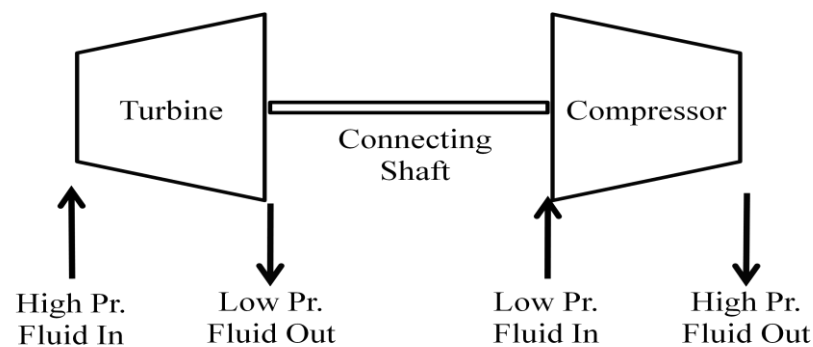
Figure 5.1 Turbine driven Compressor

The Roto-Ejector in Figure 5.3 can be compared to the Turbo-machine in Figure 5.1. It is seen that the Roto Ejector also has a turbine rotor and a compressor rotor. In our design, both the rotors (turbine and compressor) are single stage designs. They can, however, be scaled up to include multiple stages as may be feasible for the application.

The high velocity primary fluid at the exit of the nozzle is the driving fluid for the turbine. The work done by the primary fluid on the turbine is transferred to the

compressor by the connecting shaft and is used to increase the pressure of the fluid entering the compressor.

5.3   DYNAMICS OF THE ROTO-EJECTOR

Figure 5.3 shows the internal structure of a Roto- ejector. The primary fluid in the roto-ejector first expands through a supersonic nozzle (1-i^1) as in the case of a traditional ejector. At the exit of the nozzle, the fluid has reached supersonic speeds and pressures low enough to entrain a secondary fluid. At this point, before allowing the fluid to come in contact with and mix with the secondary, it is passed through a set of stationary turbine rotor blades (i^1-i). As the high velocity fluid hits the turbine blades, it causes them to spin about their axis. As this cycle gets repeated, the rotor picks up speed and starts spinning faster and faster. The rotor can be subsequently made self spinning if the blades are curved at an angle [27] and the effects of friction are minimised.

Across the nozzle, the potential energy of the fluid is converted into kinetic energy. In the rotor stage, the kinetic energy is converted into mechanical work on the shaft causing its rotation. The turbine rotors are set into motion by the change in momentum of the working fluid as it flows along the curvature of the blades.

The turbine rotor we have used in our design is an impulse stage. For an impulse rotor, the static pressure drop across the rotor blades is almost zero as can be seen from Figure 5.2. The entire pressure drop in the stage occurs across the nozzle itself.
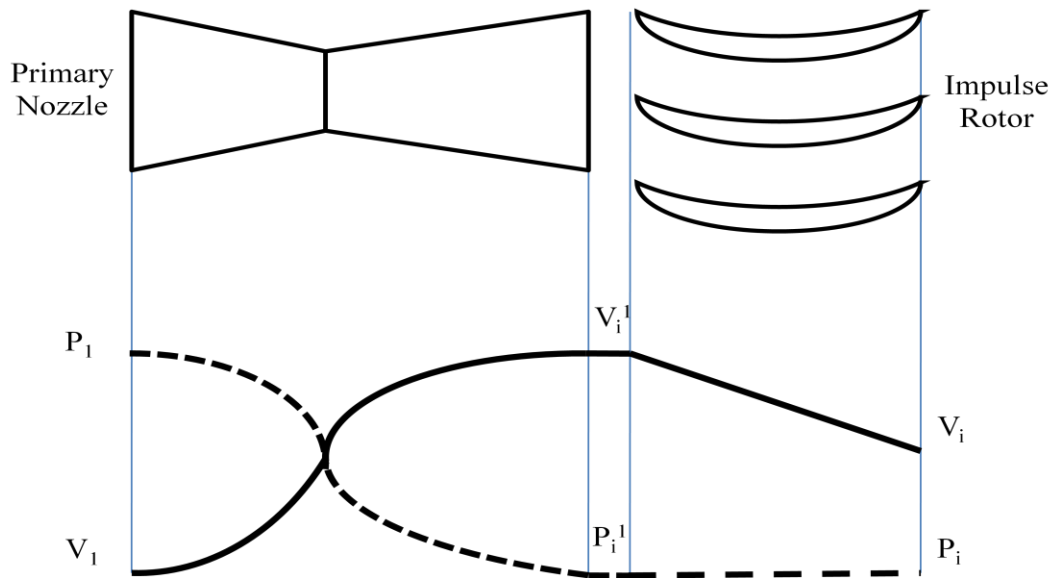
Figure 5.2 Pressure and Velocity changes in an Impulse turbine

The velocity of flow, however, increases as it flows through the nozzle and then drops across the impulse stage. As a result, the flow stagnation conditions change across the rotor stage.

To calculate the pressure, velocity and temperature of the flow at different system points in the rotor, we have used the one dimensional "Mean Line" method. When the blades are relatively short (L/D < 1/7 to 1/8), it is possible to assume that the gas pressure and the stage exit velocity do not change along the radius of the rotor. The stage is then designed considering a mean rotor radius called the "mean line". The stage is also designed in such a way that the fluid exiting the rotor stage is still supersonic to enable optimum entrainment and mixing with the secondary fluid.

As the driver primary fluid exits the turbine rotor stage, it entrains and mixes with the secondary fluid (*i-j*). The pressure of the primary fluid is the same as that at the exit of the nozzle as the pressure drop across the impulse stage is zero. The entrainment is

therefore not affected by the rotor stage. The corresponding velocity remains supersonic but is much closer to the entrained fluid's velocity. Thus the mixing is optimum and strong normal shocks are avoided.

Thus by introducing a turbine stage before mixing, we are able to recover shaft work from the fluid, bring about better mixing and avoid strong shocks while continuing to ensure that the entrainment remains optimum as desired. The recovered shaft work can be used to drive accessories like lube oil and cooling water circulation pumps or it can be used to increase the exit pressure of the handled fluid itself. We have used it for the latter case.

In the Constant Area mixing section (*j-k*), the fluids (primary and secondary) continue to mix and shock repeatedly to reach subsonic conditions. This phenomenon is the same as that which occurs in the traditional ejector. At the end of this section, the completely mixed fluid is entirely subsonic.

In the diffuser section (*k-outlet*), the pressure of the fluid increases as it flows towards the exit. Conversely the velocity reduces towards the stagnation values. This happens because the fluid is subsonic and the available cross sectional area is increased gradually. The relationship between the cross sectional area available and the variation of the fluid flow parameters are shown in Table 5.1

**Table 5.1** Variation of Nozzle Flow parameters with Cross Sectional area

IF Cross Sectional Area (A)		Sub Sonic Flow			Super Sonic Flow		
		Pressure (P)	Velocity (V)	Temperature (T)	Pressure (P)	Velocity (V)	Temperature (T)
↑	▱	↑	↓	↑	↓	↑	↓
↓	▱	↓	↑	↓	↑	↓	↑

The compressor rotor attached to the right end of the driving shaft is a single stage axial compressor. A Centrifugal compressor can also be incorporated instead of an axial stage to improve the pressure ratio but suitable thrust balancers should be introduced to neutralise or absorb the thrust loads developed. The compressor is driven by the shaft work done by the primary fluid in the turbine. No external driver is required. The speed of the compressor is the same as that of the turbine since they are coupled together. The increase in pressure in the compressor is considered to be polytropic and the relevant equations are used in calculations.

The Roto- Ejector is a vast improvement over the traditional ejector. For the same input parameters, the roto-ejector develops a considerably higher exit pressure and also has better entrainment. The higher exit pressure is achieved by utilizing the kinetic energy of the primary fluid at the nozzle exit to do useful mechanical work (drive a shaft) before it gets dissipated by turbulent mixing. A blade arrangement attached to the rotating shaft then acts as a compressor at the subsonic end of the ejector and further increases the fluid pressure.

The higher entrainment is a by-product of the above-mentioned setup. As the fluid at the exit of the nozzle flows over the turbine blades, it loses its kinetic energy to do mechanical work. So the velocity of the fluid drops while the pressure remains constant. At the turbine rotor exit, the primary fluid has a velocity much closer to that of the secondary than is achieved by the traditional ejector. As a result, the entrainment is higher, mixing is more efficient and strong shocks are avoided.

The comparison of pressures and velocities along the roto-ejector and traditional ejector are shown in the figure below
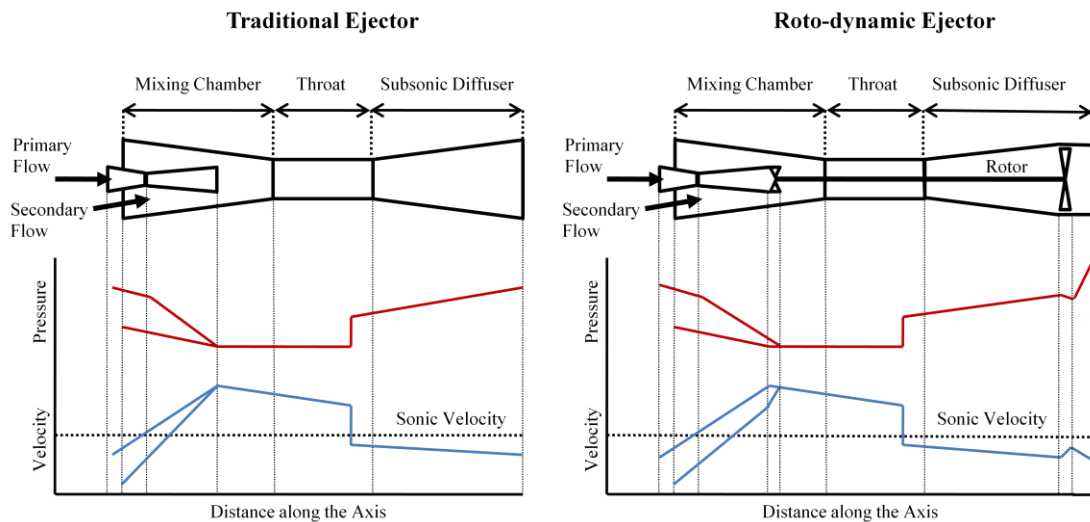
Figure 5.3 Variation of Pressure and Velocity along the length in a Traditional and Roto-dynamic Ejector

5.3   GOVERNING EQUATIONS

The governing equations used for the Roto-Ejector model are shown in this section. The following assumptions are made

1. The flow is one dimensional along the ejector and two dimensional (axial and tangential along the rotor).

2. Stagnation conditions prevail at the inlet and exit of the ejector.

3. Primary and Secondary flows are choked at the entry to the mixing chamber.

4. Except for the shocks which occur in the mixing section, the flow is isentropic.

5. The turbine rotor is approximated to an impulse stage.
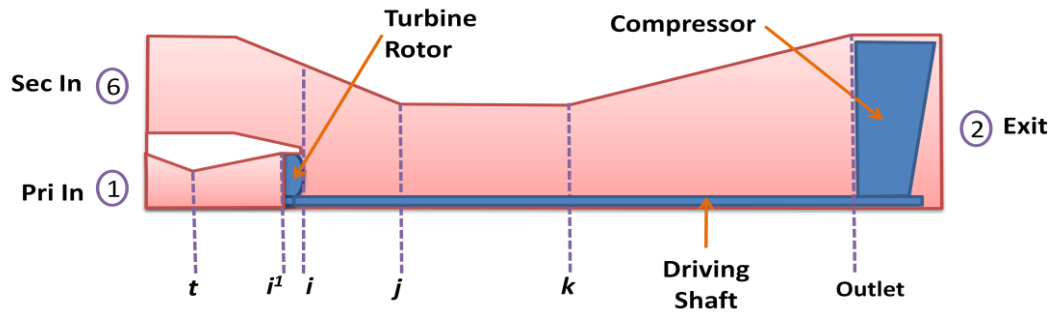
Figure 5.4 Internals of a Roto-dynamic Ejector

The inlet and outlet conditions are specified as Primary Inlet Pressure (P_{pri}) and Temperature (T_{pri}), Secondary Inlet Pressure (P_{sec}) and Temperature (T_{sec}) and Outlet Pressure (P_{out}) and Temperature (T_{out}).

The Nozzle throat diameter (D_t) is then specified.

The enthalpies at the inlets and outlet can then be calculated.

$$h_{pri} = f(T_{pri}, P_{pri}) \tag{5.1}$$

$$h_{sec} = f(T_{sec}, P_{sec}) \tag{5.2}$$

$$h_{out} = f(T_{out}, P_{out}) \tag{5.3}$$

The Mach number of the secondary fluid at section '*i*' can be calculated as

$$M_{sec-i} = \sqrt{\frac{2}{\gamma - 1}\left[\left(\frac{P_{sec}}{P_i}\right)^{\frac{\gamma-1}{\gamma}} - 1\right]} \tag{5.4}$$

Since we assume the flow to be choked, $M_{sec-i} = 1$. We can then find P_i

The Mach number of the primary fluid at the exit of the nozzle is then

$$M_{pri-i1} = \sqrt{\frac{2}{\gamma-1}\left[\left(\frac{P_{pri}}{P_i}\right)^{\frac{\gamma-1}{\gamma}}-1\right]} \qquad (5.5)$$

The Temperature of the fluid at the nozzle exit is

$$T_{pri-i1} = T_{pri}\left[1+\left(\frac{\gamma-1}{2}\right)M^2_{pri-i1}\right]^{-1} \qquad (5.6)$$

And the Velocity of the fluid is

$$V_{pri-i1} = M_{pri-i1}\sqrt{\gamma R T_{pri-i1}} \qquad (5.7)$$

The primary choking mass flow rate can also be calculated

$$\dot{m}_p = P_{pri}\left[\frac{\gamma}{R\,T_{pri}}\right]^{0.5}\left[\frac{2}{\gamma+1}\right]^{\frac{\gamma+1}{2(\gamma-1)}} \qquad (5.8)$$

The rotor behaves like a turbine and is driven by the primary fluid. The turbine Euler equation is used to solve for the unknowns.
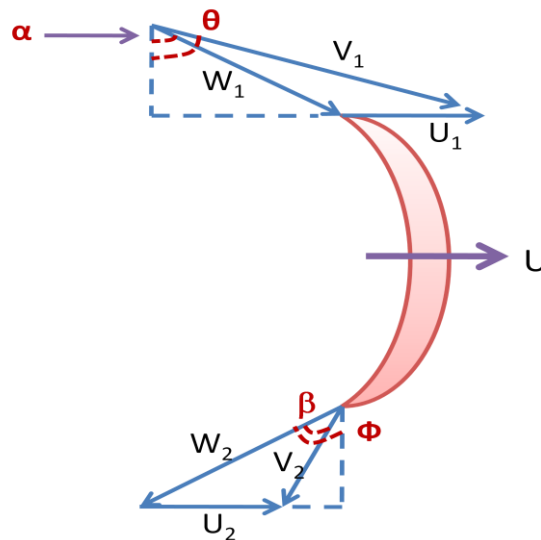
Figure 5.5 Velocity triangles for a Roto-dynamic Ejector Turbine blade

Subscript 1 = section i^I = Rotor inlet;   Subscript 2 = section i = Rotor outlet

U – Velocity of the rotor blade

V – Absolute velocity of flow

W – Relative velocity of flow

At rotor inlet,

$$V_1 = V_{pri-i1} \tag{5.9}$$

Then if the rotor speed (U) and the blade angle (θ) is specified

$$V_{u1} = V_1 \sin\theta \tag{5.10}$$

$$V_{f1} = V_1 \cos\theta \tag{5.11}$$

$$W_{u1} = V_{u1} - U_1 \tag{5.12}$$

$$W_{u1} = \sqrt{V_{f1}^2 + W_{u1}^2} \tag{5.13}$$

$$\alpha = \tan^{-1}\left[\frac{W_{u1}}{V_{f1}}\right] \tag{5.14}$$

At rotor outlet,

$$W_2 = xW_1. \quad x \text{ is the loss due to friction.}$$

$$\alpha = \beta \text{ since impulse blade.}$$

Then the outlet velocities can be calculated.

$$W_{u2} = W_2 \sin\beta \tag{5.15}$$

$$V_{f2} = W_2 \cos\beta \tag{5.16}$$

$$V_{u2} = W_{u2} - U_2 \tag{5.17}$$

$$V_2 = \sqrt{V_{u2}^2 + V_{f2}^2} \tag{5.18}$$

$$\emptyset = \tan^{-1}\left[\frac{V_{u2}}{V_{f2}}\right] \tag{5.19}$$

$$V_{pri-i} = V_2 \tag{5.20}$$

The static pressure drop across an impulse stage is zero, but due to the velocity change, the stagnation conditions will have changed.

The new stagnation conditions at the rotor exit can be calculated by the following equations

$$M_{pri-i} = \frac{V_{pri-i}}{\sqrt{\gamma R T_{pri-i}}} \tag{5.21}$$

$$To_{pri-i} = T_{pri-i} \left[1 + \left(\frac{\gamma - 1}{2} \right) M_{pri-i}^2 \right] \tag{5.22}$$

$$Po_{pri-i} = P_{pri-i} \left[1 + \left(\frac{\gamma - 1}{2} \right) M_{pri-i}^2 \right]^{\frac{\gamma}{\gamma-1}} \tag{5.23}$$

At the constant pressure mixing section, the conservation equations can be written as

Mass conservation: $\qquad\qquad m_{pri-i} + m_{sec-i} = m_j \qquad$ (5.24)

Momentum conservation: $\quad m_{pri-i} \left(V_{pri-i} \right) + m_{sec-i} \left(V_{sec-i} \right) = m_j \left(V_j \right) \quad$ (5.25)

Energy conservation: $\qquad m_{pri-i} \left(h_{pri-i} \right) + m_{sec-i} \left(h_{sec-i} \right) = m_j \left(h_j \right) \quad$ (5.26)

Sun and Eames [2] combined these equations to give

$$M_j^* = \frac{M_{pri-i}^* + \omega M_{sec-i}^* \sqrt{\frac{T_{sec}}{To_{pri-i}}}}{\sqrt{\left(1 + \omega \frac{T_{sec}}{To_{pri-i}} \right) (1 + \omega)}} \tag{5.27}$$

The relationship between M and M * is given by

$$M = \sqrt{\frac{2M_*^2}{\gamma + 1 - M_*^2(\gamma - 1)}} \tag{5.28}$$

At the constant area section, the mixed fluid experiences a shock which causes a pressure rise while reducing the velocity to subsonic condition.

The Mach No of the mixed fluid after the shock at section 'k' is given by

$$M_k = \sqrt{\frac{2 + (\gamma - 1)M_j^2}{1 + 2\gamma M_j^2 - \gamma}} \qquad (5.29)$$

Then the Pressure at section 'k' can be found by

$$P_k = \frac{P_{out}}{\left[1 + \left(\frac{\gamma - 1}{2}\right) M_k^2\right]^{\frac{\gamma}{\gamma - 1}}} \qquad (5.30)$$

P_k can be related to the area ratio $\left[\frac{A_t}{A_k}\right]$ and the entrainment ratio [ω] using the

following expression by Sun and Eames [2];

$$\frac{A_t}{A_k} = \frac{\frac{P_{out}}{Po_{pri-i}}}{\sqrt{(1 + \omega)\left(1 + \omega \frac{T_{sec}}{To_{pri-i}}\right)}} \frac{\left(\frac{P_k}{P_{out}}\right)^{\frac{1}{\gamma}} \sqrt{1 - \left(\frac{P_k}{P_{out}}\right)^{\frac{\gamma - 1}{\gamma}}}}{\left(\frac{2}{\gamma - 1}\right)^{\frac{1}{\gamma - 1}} \sqrt{1 - \frac{2}{(\gamma - 1)}}} \qquad (5.31)$$

The entrainment ratio [ω] and the Area ratio $\left[\frac{A_t}{A_k}\right]$ can be found by simultaneously

solving these equations.

The Mechanical Coefficient of performance (COP) of the cycle is then calculated by

$$COP = \frac{Q_e}{W_p} \qquad (5.32)$$

$$= \omega \left[\frac{\Delta h_e}{\Delta h_p}\right] \qquad (5.33)$$

The Power developed by the turbine rotor can be calculated if the rotor blade radius at

the inlet and outlet (r_1 and r_2) are measured.

$$\text{Power} = \frac{U}{r_m} \frac{\dot{m}_p}{g} [V_{u1} \, r_1 - V_{u2} \, r_2] \qquad (5.34)$$

If the power generated is used to further increase the pressure of the fluid, the new

exit pressure can be calculated by the following equation conservatively assuming

isentropic compression.

$$P_{exit} = P_{out} \left[1 + \left(\frac{Power}{(1 + \omega)\dot{m}_p R \, T_{out}} \right)^{\frac{\gamma - 1}{\gamma}} \right]^{\frac{\gamma}{\gamma - 1}} \tag{5.35}$$

5.4 CALCULATION SCHEME

The base model is the one discussed in Chapter III. It has been modified to predict the

performance of a roto-ejector. Turbine Euler equations have been used to solve for the

rotor parameters. The programmed code has been written in MATLAB. R134A is

used as the refrigerant fluid for the model and its thermodynamic properties have been

calculated using REFPROP. The calculation scheme followed is essentially that

shown in the previous sections. It is shown in the following flow chart for reference.
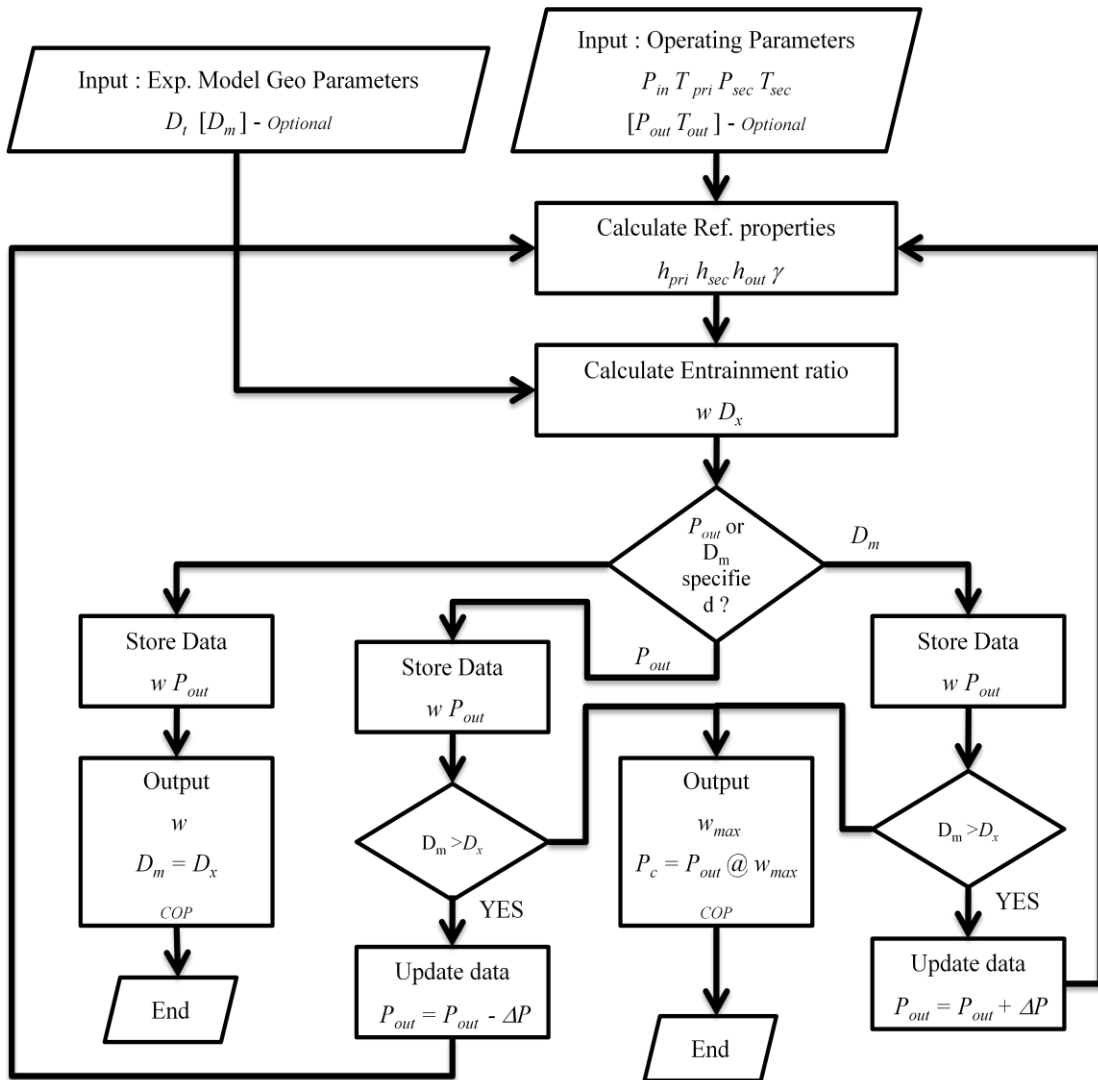
Figure 5.6 Computational Sequence of the Roto-Ejector model

The Refrigerant to be used for modelling has to be specified along with the Ejector
Primary and Secondary Inlet conditions. It is then optional to specify the Ejector
Geometric or Outlet parameters.

The model calculates the entrainment ratio, the area ratio (the ratio of the mixing
section to the throat section areas), the critical pressure and temperature and the
mechanical COP achieved.

5.5 COMPARISON OF TRADITIONAL AND ROTODYNAMIC EJECTOR PERFORMANCE

5.5.1 INTRODUCTION

The Roto-Ejector model developed to improve the ejector performance was described in previous sections. This section compares the performance of the roto ejector with that of the Ejector Driven Refrigeration System (EDRS) and basic Vapour Compression Refrigeration System (VCRS). The Roto-Ejector model will be referred to as RERS – Roto Ejector Refrigeration System. The parameters of comparison are the entrainment ratio, compression pressure ratio and COP. The refrigerant for which these comparisons are shown is R134A.

5.5.2 ENTRAINMENT RATIO OF REFRIGERANT

Entrainment ratio is defined as the ratio of the mass flow rate of the secondary to the mass flow rate of the primary fluid. Figure 5.7 shows the variation of entrainment ratios obtained by EDRS and RERS cycles with change in the condenser temperature. The evaporator temperature is held constant. The ejector nozzle throat diameter is taken as 1mm.
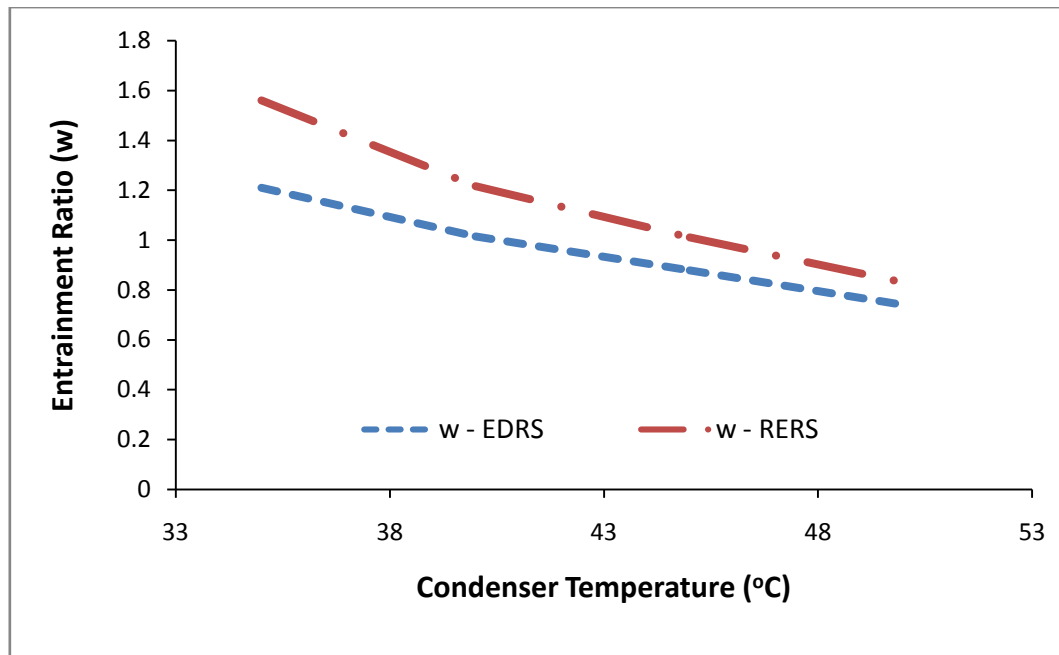
Figure 5.7 Variation of Entrainment Ratio with Condenser Temperature for

$$T_{EVAP} = 10^oC$$

The general trend for both the cycles is the same (ie; the entrainment decreases as the condenser temperature increases). It can also be seen that under similar conditions, the RERS system delivers a slightly higher rate of entrainment over the EDRS system. However the improvement seems to be higher at lower condenser temperatures (around 29% at 35 ^oC) and much lesser at higher condenser temperatures (12% at 50 ^oC).

The improved performance may be because in a RERS system, at the start of entrainment, the primary fluid's velocity is much closer to that of the secondary fluid resulting in enhanced entrainment and thorough mixing.
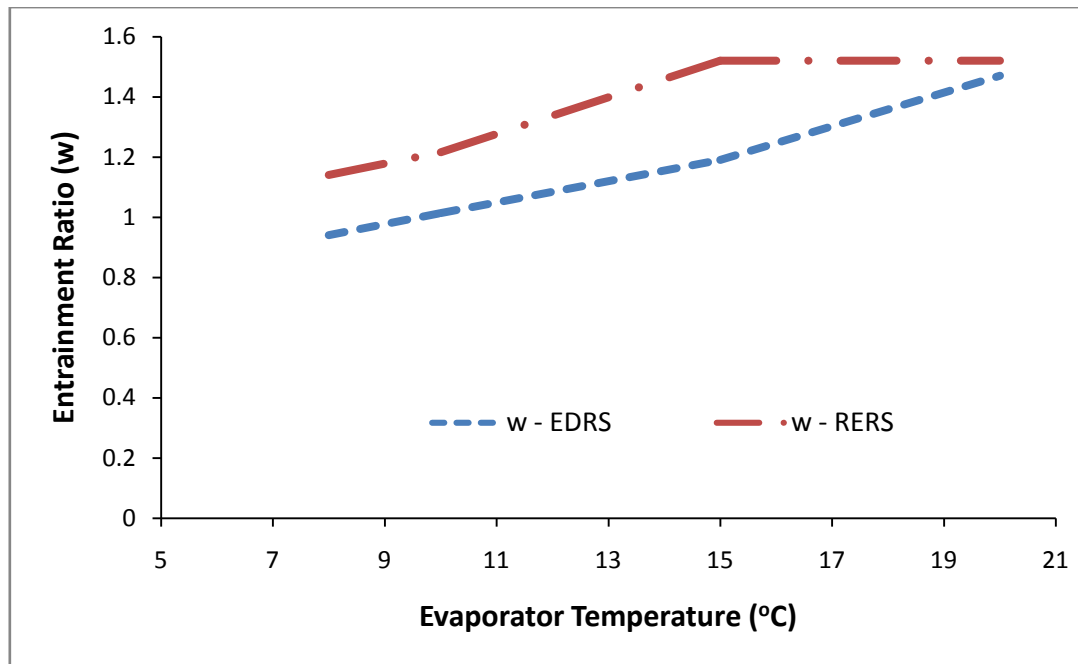
Figure 5.8 Variation of Entrainment ratio with Evaporator Temperature for

$$T_{COND} = 40^{o}C$$

The above Figure 5.8 shows the variation of Entrainment ratio with change in the Evaporator temperature. As the evaporator temperature is increased, the entrainment ratio increases up to a certain point. There after it remains constant. Under similar operating conditions, the RERS once again delivers a slightly higher entrainment when compared with EDRS. However it should also be noticed that the RERS system's entrainment peaks at a much lower Evaporator temperature value (15 ^{o}C), thus offering limited flexibility of varying this parameter.

5.5.3   COMPRESSION PRESSURE RATIO

The Pressure ratio or the pressure lift (ΔP) is the ratio of the maximum exit pressure developed by the cycle to the inlet pressure. Figure 5.9 shows the pressure ratios as a function of condenser temperatures. As the condenser temperature increases, the required pressure lift also increases.
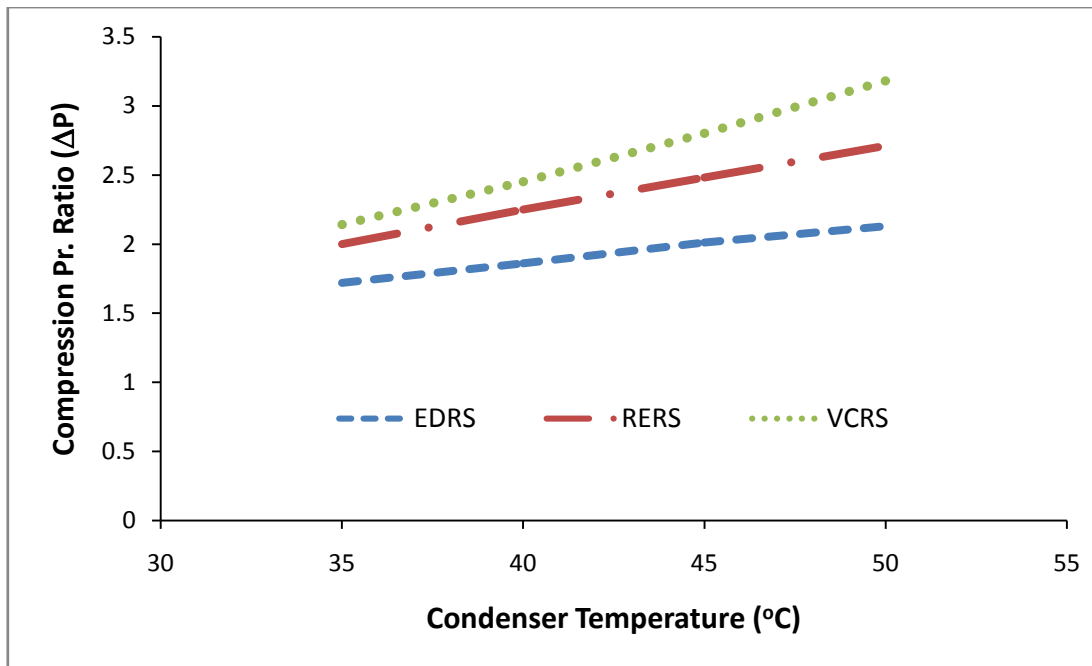
Figure 5.9 Variation of Pressure Ratio with Condenser Temperature for

$$T_{EVAP} = 10^oC$$

The maximum pressure lift is delivered by the VCRS cycle. The traditional EDRS

system is unable to match the pressure lift of VCRS and so, for successful operation,

an additional compressor should be installed to compensate for the shortfall. The

RERS system fares much better. At lower condenser temperatures, it matches the

pressure lift developed by VCRS and is capable of operating in a stand-alone mode

without any difficulty. However at higher temperatures, it does fall short and an

additional compressor must be installed to enable un-interrupted operation. However

this compressor can be of a much smaller size than that will be required for EDRS.

Figure 5.10 shows the variation of the pressure ratio with evaporator temperature. It

should be noticed that the behaviour is opposite to that of the previous section. As the

Evaporator temperature increases, the pressure ratio decreases. This is because the

evaporator belongs to the suction end of the ejector/compressor and an increase in the

evaporator temperature will increase the suction pressure, thereby reducing the

pressure ratio.
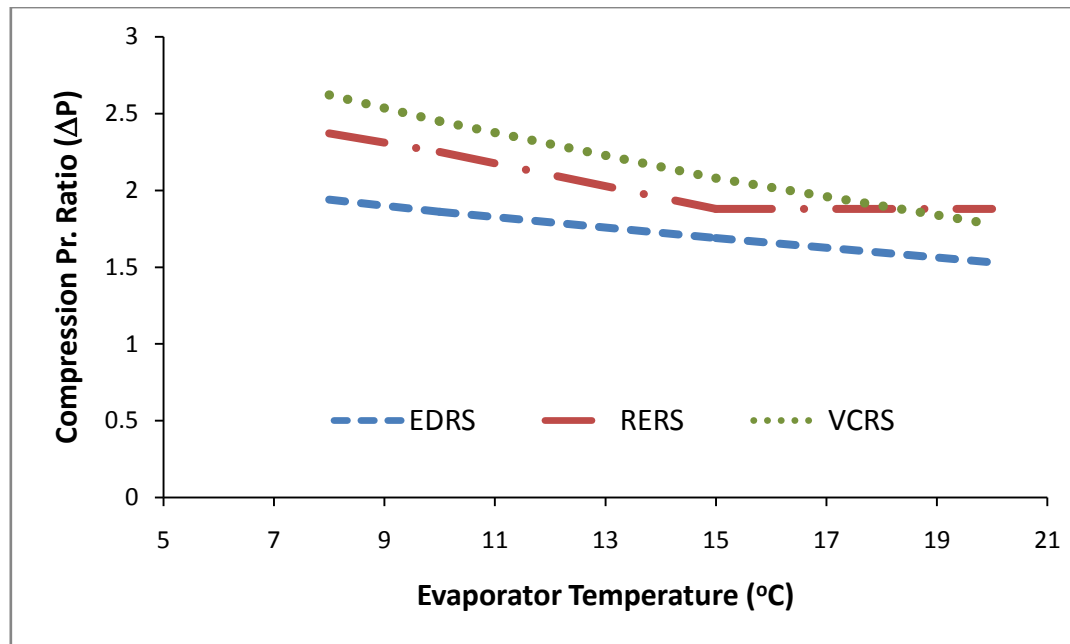
Figure 5.10 Variation of Pressure Ratio with Evaporator Temperature for

$T_{COND} = 40^{o}C$

The rest of the discussion remains unchanged. The EDRS cycle always requires an external compressor for successful operation. On the other hand, the RERS can operate without an additional driver at higher evaporator temperatures (ie; at temperatures where the RERS line slips above the VCRS line). But if lower evaporator temperatures are desired or the evaporator temperatures are expected to fluctuate widely, an additional driver will be necessary albeit of a smaller size. The improvement in pressure ratio of RERS over EDRS ranges from 11 - 27%.

5.5.4 COEFFICIENT OF PERFORMANCE (COP)

The COP of a refrigeration system is a measure of its efficiency. It can be defined as the ratio of the Refrigeration Effect developed by the system to the Mechanical work input into the system. Figure 5.11 shows the variation of COP with change in Evaporator temperature.
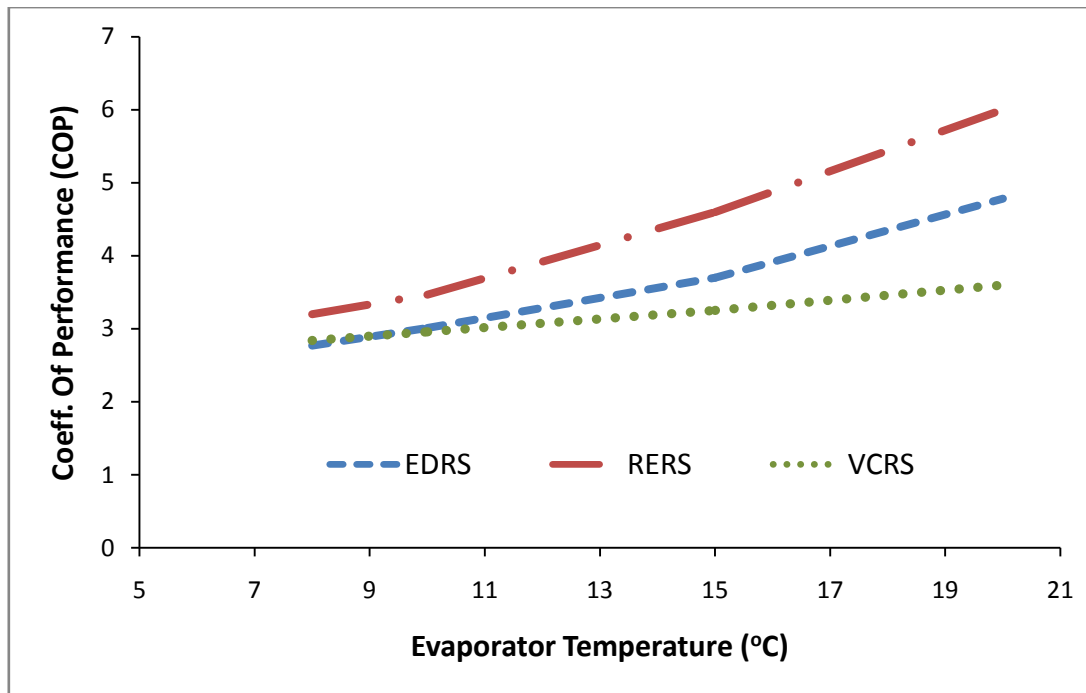
Figure 5.11 Variation of COP with Evaporator Temperature for

$T_{COND} = 40^oC$

It is seen that as the Evaporator temperature is increased, the COP increases

irrespective of the cycle. This is because a higher Evaporator temperature will result

in a higher compressor suction pressure. So the pressure lift required is lesser

resulting in reduced compressor work.

Across the cycles, it should be noticed that both EDRS and RERS perform better than

the VCRS cycle. The COP improvement of EDRS over VCRS ranges from 0 – 30%.

This result is in line with that of Sarkar [9], Menegay and Kornhauser [8],

Chaiwongsa and Wongwises [7]. The COP improvement of RERS over VCRS ranges

from 12 – 60 %.

CHAPTER VI

SUMMARY AND CONCLUSIONS

6.1   SUMMARY

Ejectors are devices which have the potential to replace the existing Vapour Compression systems for use in refrigeration and air conditioning applications. They have the advantage of being simple to design, construct and operate compared to vapour compression systems which have a lot of mechanical components. They also do not require a externally powered driver like the compressor. A comprehensive theoretical study of the ejector energy and momentum transfer was carried out and the basic concepts and the governing equations were introduced. On their basis a one dimensional model was developed.

Effort was devoted to validating the performance of the model for constant pressure and constant area operation. The model was also validated by comparing the performance with that obtained by numerous researchers in their experimental models. It was further tested for robustness by testing its prediction for different refrigerants.

Two issues related to Ejector Driven Systems were dealt with. The first is "Alternate Refrigerant Prediction". The validated model was used to choose the best alternate refrigerant if refrigerant replacement is to be done. This is important as most ejector systems currently in operation have been designed for CFCs and HCFCs which are now banned / restricted. Our model can predict the performance of any refrigerant if

the desired refrigerant and existing model's geometric parameters are fed in. In this thesis, the model has been used to predict alternates for R11, R123 and R141b. But performance of any refrigerant or mixture in the REFPROP database can be modelled. We find that when higher operating pressures can be tolerated, Ammonia and R134a pose as very good replacement alternatives for the base refrigerants considered. Both these refrigerants develop a much higher entrainment ratio and COP when compared with the base refrigerant. When systems have not been designed to handle very high pressures, R245fa or R245ca may be considered as replacements. They entrain slightly lesser than the base refrigerants but have very similar operating pressures and temperatures.

The other issue addressed in this thesis is "Performance Improvement of the Cycle". To achieve this aim, a novel "Roto-Dynamic Ejector" was introduced. A complete treatise of the concept and governing equations was given. A model was developed based on the governing equations. The performance of the model was then compared with that of the basic Ejector Driven and Vapour Compression cycles. R134a was used as the refrigerant in this thesis, but the performance of any other refrigerant can also be modelled. The improvements in performance have then been discussed.

6.2   BENEFITS OF USING A ROTO – EJECTOR

The Roto – Ejector is a novel concept. It is an improvement over the Ejector Driven Refrigeration System (EDRS) and poses as a more attractive environment friendly alternative to conventional Vapour Compression Refrigeration System (VCRS).

Based on our model predictions, for refrigerant R134a, the following improvements over the traditional ejector systems have been computed

12 – 29 % improvement in entrainment

0 – 30 % improvement in COP

11 - 27% improvement in pressure ratio.

Other benefits of using a roto-ejector instead of traditional ejectors include a wider permissible range of operation resulting in greater flexibility of usage, reduced capital costs due to smaller compressor sizes required and minimal requirement of external power source / driver resulting in reduced operating costs as well.

6.3   RECOMMENDATIONS FOR FUTURE WORK

Based on our model predictions, it has been shown that Roto-Ejector systems perform better and deliver a higher COP than traditional Ejector systems. However the intention of this thesis was only to show that this is a feasible option to consider for improving ejector performances. Issues like the complexities in the rotor geometry, thrust load vectoring and balancing, effect of rotor multi-staging, parametric response to shock loading and process flow surges, rotor rigidity, torsional and frequency analysis have not been considered.

A researcher interested in building on this work will have to build a more robust model considering all these factors if the intention is to mimic a similar physical model as closely as possible.

Alternately, building a physical model and carrying out analysis to establish the deviation in performance from the computational model can be done to assess the effect of unconsidered / unresolved forces and conditions on the performance.

The rotor we have used has a single turbine and a single compressor stage. Researchers can explore options in multistaging the rotor and studying its effect on the performance.

The torque or power developed by the turbine rotor is directly proportional to the mean radius of the turbine blade arrangement measured from the axis of rotation. By shifting the primary nozzle to the periphery of the ejector, for the same fluid quantity and operating conditions, the power developed by the turbine rotor will be much higher resulting in even better performance.

Also instead of a single primary nozzle, an array of nozzles spread around the circumference could be used for evenly distributing the torque developed throughout the cycle and minimizing thrust balancing requirements. These options can be explored as subjects of future research work.

BIBLIOGRAPHY

[1]   Keenan, J. H., Neumann, E. P., and Lustwerk, F., 1950, "An Investigation of Ejector Design by Analysis and Experiment," J Appl Mech-T Asme, 17(3), pp. 299-309.

[2]   Sun, D. W., and Eames, I. W., 1996, "Performance characteristics of HCFC-123 ejector refrigeration cycles," Int J Energ Res, 20(10), pp. 871-885.

[3]   Huang, B. J., and Chang, J. M., 1999, "Empirical correlation for ejector design," Int J Refrig, 22(5), pp. 379-388.

[4]   Sriveerakul, T., Aphornratana, S., and Chunnanond, K., 2007, "Performance prediction of steam ejector using computational fluid dynamics: Part 1. Validation of the CFD results," International Journal of Thermal Sciences, 46(8), pp. 812-822.

[5]   Sriveerakul, T., Aphornratana, S., and Chunnanond, K., 2007, "Performance prediction of steam ejector using computational fluid dynamics: Part 2. Flow structure of a steam ejector influenced by operating pressures and geometries," International Journal of Thermal Sciences, 46(8), pp. 823-833.

[6]   Pianthong, K., SeehanaM, W., Behnia, M., SriveerakUl, T., and Aphornratana, S., 2007, "Investigation and improvement of ejector refrigeration system using computational fluid dynamics technique," Energy Conversion and Management, 48(9), pp. 2556-2564.

[7]   Chaiwongsa, P., and Wongwises, S., 2008, "Experimental study on R-134a refrigeration system using a two-phase ejector as an expansion device," Appl Therm Eng, 28(5-6), pp. 467-477.

[8]   Menegay, P., and Kornhauser, A. A., 1996, "Improvements to the ejector expansion refrigeration cycle," Proc Iecec, pp. 702-706.

[9]   Sarkar, J., 2010, "Geometric parameter optimization of ejector-expansion refrigeration cycle with natural refrigerants," Int J Energ Res, 34(1), pp. 84-94.

[10]   Zare-Behtash, H., Gongora-Orozco, N., and Kontis, K., 2011, "Effect of primary jet geometry on ejector performance: A cold-flow investigation," International Journal of Heat and Fluid Flow, 32(3), pp. 596-607.

[11]   Ruangtrakoon, N., Aphornratana, S., and Sriveerakul, T., 2011, "Experimental studies of a steam jet refrigeration cycle: Effect of the primary nozzle geometries to system performance," Exp Therm Fluid Sci, 35(4), pp. 676-683.

[12]   Cizungu, K., Groll, M., and Ling, Z. G., 2005, "Modelling and optimization of two-phase ejectors for cooling systems," Appl Therm Eng, 25(13), pp. 1979-1994.

[13]   Huang, B. J., Wu, J. H., Yen, R. H., Wang, J. H., Hsu, H. Y., Hsia, C. J., Yen, C. W., and Chang, J. M., 2011, "System performance and economic analysis of solar-assisted cooling/heating system," Sol Energy, 85(11), pp. 2802-2810.

[14]   Huang, B. J., Petrenko, V. A., Chang, J. M., Lin, C. P., and Hu, S. S., 2001, "A combined-cycle refrigeration system using ejector-cooling cycle as the bottom cycle," Int J Refrig, 24(5), pp. 391-399.

[15]   Diaconu, B. M., 2012, "Energy analysis of a solar-assisted ejector cycle air conditioning system with low temperature thermal energy storage," Renewable Energy, 37(1), pp. 266-276.

[16]   Wang, F., and Shen, S. Q., 2010, "Energy and exergy analysis of novel solar bi-ejector refrigeration system with injector," Int J Energ Res, 34(9), pp. 815-826.

[17]   Elbel, S., 2011, "Historical and present developments of ejector refrigeration systems with emphasis on transcritical carbon dioxide air-conditioning applications," Int J Refrig, 34(7), pp. 1545-1561.

[18]   Huang, B. J., Chang, J. M., Wang, C. P., and Petrenko, V. A., 1999, "A 1-D analysis of ejector performance," Int J Refrig, 22(5), pp. 354-364.

[19]   Hirotsugu Takeuchi, Y. K., Hiroshi Oshitani, Gota Ogata, 2001, "Ejector cycle system," USPTO, ed., Denso Corporation, United States.

[20]   Hirotsugu Takeuchi, S. N., 2003, "Vehicle air conditioner with ejector refrigerant cycle," U. S. Patent, ed., DENSO Corporation, United States.

[21]   Hiroshi Oshitani, Y. Y., Hirotsugu Takeuchi, Katsuya Kusano, Makoto Ikegami, Yoshiaki Takano, Naohisa Ishizaka, Takayuki Sugiura, Aug 14, 2007, "Vapor compression cycle having ejector," U. S. Patent, ed., DENSO Corporation (Kariya, JP) United States.

[22]   Chunnanond, K., and Aphornratana, S., 2004, "An experimental investigation of a steam ejector refrigerator: the analysis of the pressure profile along the ejector," Appl Therm Eng, 24(2-3), pp. 311-322.

[23]   Varga, S., Oliveira, A. C., and Diaconu, B., 2009, "Influence of geometrical factors on steam ejector performance – A numerical assessment," International Journal of Refrigeration, 32(7), pp. 1694-1701.

[24]   ASHRAE Handbook, ed., 1983, Equipments Volume, American Society of Heating, Refrigeration and Air- Conditioning Engineers, Atlanta, GA 30329, pp.13.1-13.6.

[25]   Ouzzane, M., and Aidoun, Z., 2003, "Model development and numerical procedure for detailed ejector analysis and design," Appl Therm Eng, 23(18), pp. 2337-2351.

[26]   Sarkar, J., 2009, "Performance characteristics of natural-refrigerants-based ejector expansion refrigeration cycles," P I Mech Eng a-J Pow, 223(A5), pp. 543-550.

[27]   Foa, J. V., 1962, "Method of Energy exchange and Apparatus to carry out the same," USPTO, ed., Research Corporation, New York, United States.

[28]   Yapici, R., Ersoy, H. K., Aktoprakoglu, A., Halkaci, H. S., and Yigit, O., 2008, "Experimental determination of the optimum performance of ejector refrigeration system depending on ejector area ratio," Int J Refrig, 31(7), pp. 1183-1189.

[29]   Hsu, C. T., 1984, "Investigation of an Ejector Heat Pump by Analytical Methods," Oak Ridge National Laboratory, Tennessee.

[30]   Selvaraju, A., and Mani, A., 2006, "Experimental investigation on R134a vapour ejector refrigeration system," Int J Refrig, 29(7), pp. 1160-1166.

[31]   Sun, D. W., 1997, "Solar powered combined ejector vapour compression cycle for air conditioning and refrigeration," Energy Conversion and Management, 38(5), pp. 479-491.

[32]   Anonymous, 2011, ""Refrigerant"," Wikipedia, the free encyclopedia.

[33]   Tyagi, K. P., and Murty, K. N., 1985, "Ejector Compression Systems for Cooling - Utilizing Low-Grade Waste Heat," J Heat Recov Syst, 5(6), pp. 545-550.

[34]   Chen, F. C., and Hsu, C. T., 1987, "Performance of Ejector Heat-Pumps," Int J Energ Res, 11(2), pp. 289-300.

[35]   Nahdi, E., Champoussin, J. C., Hostache, G., and Cheron, J., 1993, "Optimal Geometric Parameters of a Cooling Ejector-Compressor," Int J Refrig, 16(1), pp. 67-72.

[36]   Manzer, L. E., 1990, "The CFC-ozone issue: Progress on the development of alternatives to CFCs.," Science, 249, pp. 31-35.

[37]   Charles A Garris, J., 2009, "Pressure Exchange Ejector," USPTO, ed., George Washington University, United States.

APPENDIX A

SAMPLE MATLAB CODE FOR 1D EJECTOR MODEL

```
% TWO PHASE EJECTOR MODEL

% Waste heat from Gen is not reqd for cycle to operate.
% Can be coupled to VCRS to reduce Comp load and improve Mech COP.

% Ejec Pri inlet is sat liquid and Sec inlet is sat vapour.
% 1 - Cond Out and Ejec Pri In
% 2 - Ejec Out
% 3 - Comp In
% 4 - Comp Out
% 3' - Exp Valve In
% 5 - Exp Valve Out
% 6 - Evap Out and Ejec Sec In

% Nozzle throat area is assumed to be one m2 (unit area)

% INPUTS

F = 'R134A'; % Refrigerant fluid
At =(3.14/4)*(0.001)^2; % Unit throat area
Am =(3.14/4)*(0.00235)^2; % Mixing Section area
T1 = 40+273; % Condenser Exit or Ejec Pri Inlet Temp (Kelvin)
T6 = 8+273; % Evaporator Exit or Ejec Sec Inlet Temp (Kelvin)
Eff = 0.85; % Nozzle Efficiency
DOSC = 2 ; % Degree of subcooling
DOSH = 2 ; % Degree of superheating

P1 = refpropm('P','T',T1-DOSC,'Q',0,F); % KPa
P1 = P1*10^3; % Pa

P6 = refpropm('P','T',T6,'Q',1,F);
P6 = P6*10^3;

% 1. Calculate state enthalpies
[h1 s1] = refpropm('HS','T',T1-DOSC,'P',P1*10^-3,F);
h6 = refpropm('H','T',T6,'Q',1,F);

% 2. Calculate Gas constants
Gamma1 = refpropm('K','T',T6,'Q',1,F);
Gamma2 = refpropm('K','T',T1-DOSC,'Q',0,F);
Gamma = (Gamma1 + Gamma2)/2;

Ak = Am+1;
T2 = T6;
while Ak > Am ;
    T2 = T2+0.1;

P2 = refpropm('P','T',T2,'Q',1,F);
P2 = P2*10^3;

%%% ASSUMPTIONS
```

```
% Isentropic flow in Nozzle, Mixing chamber on either side of shock,
%   and Diffuser.
% Double choked condition - Pri & Sec flows are choked at entry to mixing chamber.
% Gamma is the value at secondary inlet, since it doesn't change much.


% 1D analysis for ejector

% 3. Calculate Pi
M6i = 1 ;
Pi = P6;
ERR_1 = 1;

while ERR_1 > 0.01;
   Pi = Pi - 1;
   RHS_1 = sqrt((2/(Gamma-1))*((P6/Pi)^((Gamma-1)/Gamma)-1));
   ERR_1 = abs(RHS_1 - M6i);
end




% 4. Calculate M1ix
M1i = Eff*sqrt((2/(Gamma-1))*((P1/Pi)^((Gamma-1)/Gamma)-1));

Pj = Pi; % Const Pr. mixing

% 5. Check for double choked condition
if M1i > 1 ;

% 6. Calculate parameters across shock
Mj = M1i;
ERR_2 = 10^6;

while ERR_2 > 0.01;
   Mj = Mj - 0.001;
   LHS_2 = P2/((1+(((Gamma-1)/2)*((2+(Gamma-1)*(Mj^2))/(1+(2*Gamma*(Mj^2))-
Gamma))))^(Gamma/(Gamma-1)));
   X1 = sqrt((2+((Mj^2)*(Gamma-1)))/(2+(((2+((Gamma-1)*(Mj^2)))/(1+(2*Gamma*(Mj^2))-
Gamma))*(Gamma-1))));
   RHS_2 = (Pj*Mj*X1)/(sqrt((2+((Gamma-1)*(Mj^2)))/(1+(2*Gamma*(Mj^2))-Gamma)));
   ERR_2 =(RHS_2 - LHS_2);
end

Pk = LHS_2;
Mk = sqrt((2+(Gamma-1)*(Mj^2))/(1+(2*Gamma*(Mj^2))-Gamma));

% 7. Calculate parameters across mixing section before shock

% Mm1i
Mm1i = 1 ;
ERR_3 = 1;

while ERR_3 > 0.01;
   Mm1i = Mm1i + 0.001;
   RHS_3 = sqrt((2*Mm1i^2)/(Gamma+1-((Mm1i^2)*(Gamma-1))));
   ERR_3 = abs(RHS_3 - M1i);
end
```

```
% Mm6i
Mm6i = 0.999 ;
ERR_4 = 1;

while ERR_4 > 0.01;
    Mm6i = Mm6i + 0.001;
    RHS_4 = sqrt((2*Mm6i^2)/(Gamma+1-((Mm6i^2)*(Gamma-1))));
    ERR_4 = abs(RHS_4 - M6i);
end


% Mmj
Mmj = 0.999 ;
ERR_5 = 1;

while ERR_5 > 0.01;
    Mmj = Mmj + 0.001;
    RHS_5 = sqrt((2*Mmj^2)/(Gamma+1-((Mmj^2)*(Gamma-1))));
    ERR_5 = abs(RHS_5 - Mj);
end


% 8. Calculate Entrainment ratio
w1 = 0.01;
ERR_7 = 1;

while ERR_7 > 0.01;
    w1 = w1 + 0.001;
    RHS_7 = (Mm1i + w1*Mm6i*sqrt(T6/(T1-DOSC)))/(sqrt((1+(w1*T6/(T1-DOSC)))*(1+w1)));
    ERR_7 = abs(RHS_7 - Mmj);
end


% 9. Calculate Mixing Section CS area
X2 = (P2/P1)/(sqrt((1+w1)*(1+(w1*T6/(T1-DOSC)))));
X3 = (((Pk/P2)^(1/Gamma))*sqrt(1-(Pk/P2)^((Gamma-1)/Gamma)));
X4 = ((2/(Gamma+1))^(1/(Gamma-1)))*sqrt(1-(2/(Gamma+1)));
Eff1 = 0.83;


Ak = (1/(Eff1^2))*At*X4/(X2*X3);


Dk = sqrt(Ak*4/3.14);
display([Dk])
else
    display(['Rotor exit is not supersonic. Increase P1/T1 or change rotor dimensions'])
end
end


% 10. Find Nozzle Choking mass flow rate
Qt = refpropm('Q','P',((1+(Gamma-1)/2)^(-Gamma/(Gamma-1)))*P1*10^-3,'S',1.05*s1,F);


Atl = refpropm('A','P',((1+(Gamma-1)/2)^(-Gamma/(Gamma-1)))*P1*10^-3,'Q',0,F);
Atv = refpropm('A','P',((1+(Gamma-1)/2)^(-Gamma/(Gamma-1)))*P1*10^-3,'Q',1,F);
D1 = refpropm('D','P',((1+(Gamma-1)/2)^(-Gamma/(Gamma-1)))*P1*10^-3,'Q',Qt,F);
A1 = (Qt*Atv)+((1-Qt)*Atl);


mp = D1*A1*At ; % kg/s


% 11. Calculate Compressor Work
T3 = refpropm('T','P',P2*10^-3,'Q',1,F);
```

```
T3i = refpropm('T','P',P2*10^-3,'Q',0,F);

[h3 s3] = refpropm('HS','T',T3+DOSH,'P',P2*10^-3,F);
h3i = refpropm('H','P',P2*10^-3,'Q',0,F);

[h4 T4] = refpropm('HT','P',P1*10^-3,'S',1.05*s3,F);

WD = mp*(1/Eff)*(h4-h3); % KW

CC = w1*mp*Eff*(h6-1.05*h3i);

% 12. Calculate COP
COPm_1 = CC/WD; %w2*(h6-h3)/(h4-h3); % Mechanical COP:(Ref Effect/Mech Work Done)


% 13. Display Results
display(['2P Ejector Model'])
display(['w   COPm   Ak(m2)'])
display([w1 COPm_1 Ak])
```

APPENDIX B

SAMPLE MATLAB CODE FOR ROTO - EJECTOR MODEL

```
%%% TO FIND w, COP & Power FOR A ROTO-EJECTOR SYSTEM

% Program to calculate Entrainment ratio, COP and Power developed
% by an roto ejector if Inlet and outlet Press and Temp are specified along
% with Nozzle throat area.
% Rotor dimensional parameters also have to be specified.

% Primary fluid path: Ejector Out-Comp-Gen-Ejec Primary In
% Sec fluid path: Ejector Out-Comp-Cond-Exp valve-Ejec Sec in

%%% CONVENTIONS

% 1 - Pri Inlet
% 2 - Diff Exit
% 6 - Sec Inlet
% t - Noz throat
% i'- Noz exit (Rotor Inlet)
% i - Rotor exit
% j - Start of Const area mixing chamber
% k - End of Const area mixing chamber

% P - Pressure
% T - Temperature
% h - Enthalpy
% w - Entrainment ratio (ms/mp)


%%% INPUTS
theta = 60; % degrees % Rotor absolute flow inlet angle
N = 10050; % rpm % Rotor speed
r1 = sqrt(4*At/3.14); % m % Rotor mean radius at inlet
r2 = sqrt(4*At/3.14); % m % Rotor mean radius at exit
f = 0.9; % Rotor blade friction factor

%%% ASSUMPTIONS

% Isentropic flow in Nozzle, Mixing chamber on either side of shock,
%   and Diffuser.
% Double choked condition - Pri & Sec flows are choked at entry to mixing chamber.
% Gamma is the value at secondary inlet, since it doesn't change much.
% 1D analysis for ejector

% 2D analysis for rotor (axial and tangential directions)
% Static Pr and T drop across the turbine blade is negligible (Impulse
% blade)
% Relative flow inlet angle (alpha) is equal to the relative flow exit
% angle (beta)

T1 = Tg; % Kelvin
P1 = refpropm('P','T',T1,'Q',1,F); % KPa
P1 = P1*10^3; % Pa

T2 = Tc;
```

```
P2 = refpropm('P','T',T2,'Q',1,F);
P2 = P2*10^3;


T6 = Te;
P6 = refpropm('P','T',T6,'Q',1,F);
P6 = P6*10^3;



% 1. Calculate Gas constants
Gamma = refpropm('K','T',T6,'P',P6*10^-3,F);

[C1 O1] = refpropm('CO','T',T6,'P',P6*10^-3,F);
R = C1-O1; % J/Kg-K

% 2. Calculate Pi
M6i = 1 ;
Pi = P6;
ERR_1 = 1;

while ERR_1 > 0.01;
    Pi = Pi - 1;
    RHS_1 = sqrt((2/(Gamma-1))*((P6/Pi)^((Gamma-1)/Gamma)-1));
    ERR_1 = abs(RHS_1 - M6i);
end

% 3. Calculate state enthalpies
h1 = refpropm('H','T',T1,'P',P1*10^-3,F);
h2 = refpropm('H','T',T2,'P',P2*10^-3,F);
h6 = refpropm('H','T',T6,'P',P6*10^-3,F);

[h2 s2] = refpropm('HS','P',P2*10^-3,'Q',1,F);
h3 = refpropm('H','P',P1*10^-3,'S',s2,F);

% 4. Calculate M1ix
M1ix = sqrt((2/(Gamma-1))*((P1/Pi)^((Gamma-1)/Gamma)-1));

% 5. Find Vix
T1ix = T1 * (1+((Gamma-1)/2*(M1ix)^2))^(-1);
A1ix = refpropm('A','T',T1ix,'P',Pi*10^-3,F);
V1ix = M1ix * A1ix;

% 6. Calculate rotor inlet turbo parameters
V1 = V1ix;
u1 = r1*(2*3.14*N/60);

Vu1 = V1 * sin(theta*3.14/180);
Vf1 = V1 * cos(theta*3.14/180);
Wu1 = Vu1 - u1;
W1 = sqrt((Vf1)^2 + (Wu1)^2);
alpha = atan(180/3.14*Wu1/Vf1);

% 7. Calculate rotor exit turbo parameters
W2 = f*W1;
beta = alpha;
u2 = r2*(2*3.14*N/60);

Wu2 = W2 * sin(beta*3.14/180);
Vf2 = W2 * cos(beta*3.14/180);
Vu2 = Wu2 - u2;
V2 = sqrt((Vu2)^2 + (Vf2)^2);
```

```
psi = atan(180/3.14*Vu2/Vf2);

V1i = V2;

% 8. Calculate mach no at rotor exit
T1i = T1ix ; % since Impulse blade ??
Cp = refpropm('C','T',T1i,'P', Pi*10^-3,F);

To1i = ((V1i)^2)/(2*9.81* Cp)+ T1i ; % obsolete
Po1i = Pi * ((To1i/T1i)^(Gamma/(Gamma-1))); % obsolete
M1i = sqrt((2/(Gamma-1))*((To1i/T1i)-1)); % Obsolete

A1i = refpropm('A','T',T1i,'P',Pi*10^-3,F);
M1i = Eff* V1i / A1i;

% New stagnation conditions
To1i = T1i*(1+(Gamma-1)/2*M1i^2);
Po1i = Pi * ((To1i/T1i)^(Gamma/(Gamma-1)));

Pj = Pi; % Const Pr. mixing

% 9. Check for double choked condition
if M1i > 1 ;

% 10. Calculate parameters across shock
Mj = M1i;
ERR_2 = 10^6;

while ERR_2 > 0.01;
    Mj = Mj - 0.001;
    LHS_2 = P2/((1+(((Gamma-1)/2)*((2+(Gamma-1)*(Mj^2))/(1+(2*Gamma*(Mj^2))-
Gamma))))^(Gamma/(Gamma-1)));
    X1 = sqrt((2+((Mj^2)*(Gamma-1)))/(2+(((2+((Gamma-1)*(Mj^2)))/(1+(2*Gamma*(Mj^2))-
Gamma))*(Gamma-1))));
    RHS_2 = (Pj*Mj*X1)/(sqrt((2+((Gamma-1)*(Mj^2)))/(1+(2*Gamma*(Mj^2))-Gamma)));
    ERR_2 =(RHS_2 - LHS_2);
end

Pk = LHS_2;
Mk = sqrt((2+(Gamma-1)*(Mj^2))/(1+(2*Gamma*(Mj^2))-Gamma));

% 11. Calculate parameters across mixing section before shock

% Mm1i
Mm1i = 1 ;
ERR_3 = 1;

while ERR_3 > 0.01;
    Mm1i = Mm1i + 0.001;
    RHS_3 = sqrt((2*Mm1i^2)/(Gamma+1-((Mm1i^2)*(Gamma-1))));
    ERR_3 = abs(RHS_3 - M1i);
end

% Mm6i
Mm6i = 0.999 ;
ERR_4 = 1;

while ERR_4 > 0.01;
    Mm6i = Mm6i + 0.001;
    RHS_4 = sqrt((2*Mm6i^2)/(Gamma+1-((Mm6i^2)*(Gamma-1))));
```

```
      ERR_4 = abs(RHS_4 - M6i);
   end


% Mmj
Mmj = 0.999 ;
ERR_5 = 1;

while ERR_5 > 0.01;
   Mmj = Mmj + 0.001;
   RHS_5 = sqrt((2*Mmj^2)/(Gamma+1-((Mmj^2)*(Gamma-1))));
   ERR_5 = abs(RHS_5 - Mj);
end

% 12. Calculate Entrainment ratio
w2 = 0.01;
ERR_7 = 1;

while ERR_7 > 0.01;
   w2 = w2 + 0.001;
   RHS_7 = (Mm1i + w2*Mm6i*sqrt(T6/To1i))/(sqrt((1+(w2*T6/To1i))*(1+w2)));
   ERR_7 = abs(RHS_7 - Mmj);
end

% 13. Find Nozzle Choking mass flow rate
[D1 A1] = refpropm('DA','T',(1/(1+(Gamma-1)/2))*T1,'P',((1+((Gamma-1)/2)^(-(Gamma-
1)/Gamma))^-1)*P1*10^-3,F);
mp = D1*A1*At ; % kg/s

% 14. Calculate Power developed by turbine
Pow = (2*3.14*N/60)*(mp)*((Vu1*r1)-(Vu2*r2)); % Watts

% 15. Calculate Mixing Section CS area
X2 = (P2/Po1i)/(sqrt((1+w2)*(1+(w2*T6/To1i))));
X3 = (((Pk/P2)^(1/Gamma))*sqrt(1-(Pk/P2)^((Gamma-1)/Gamma)));
X4 = ((2/(Gamma+1))^(1/(Gamma-1)))*sqrt(1-(2/(Gamma+1)));

Akr = At*X4/(X2*X3);

Dkr = sqrt(Akr*4/3.14);

% 16. Calculate auxiliary compressor parameters

% ie Pr rise possible if power generated is used for further compression
% Isentropic compression
P7 = P2*((1+(Pow/((1+w2)*mp*R*T2))*((Gamma-1)/Gamma))^(Gamma/(Gamma-1)));

% 17. Calculate Compressor Work
h5 = h6-(CC/(w2*mp));
h4 = h5;

WP4 = (1+w2)*mp*(h3-h2); % W

% 16. Calculate COP
COPm_4 = CC/WP4; % Mech COP
COPt_4 = CC/(WP4+(mp*(h1-h3))); % Thermal COP

else
   display(['Rotor exit is not supersonic. Increase P1/T1 or change rotor dimensions'])
end
```

APPENDIX C

SAMPLE MATLAB CODE FOR A VCRS MODEL

```matlab
% Program for simulating States and COP of a Vap Comp Ref Cycle

% INPUTS
Tc = Tc1; % Cond/outside Temp (K)
DSh = 2; % Degree of Superheat at Comp Inlet (K)
DSc = 2; % Degree of Subcool at Cond Outlet (K)

% STATES

% 6-2 Compressor (Isentropic)
% 2-3 Condenser (Isobaric)
% 3-5 Expansion (Isenthalpic)
% 5-6 Evaporation (Isobaric)

% Point 6
P6 = refpropm('P','T',Te,'Q',1,F);
P6 = P6 *10^3; % Pa
T6 = Te + DSh; % K
S6 = refpropm('S','T',T6,'P',P6*10^-3,F); % J/Kg-K
H6 = refpropm('H','T',T6,'P',P6*10^-3,F); % J/Kg

% Point 3
P3 = refpropm('P','T',Tc,'Q',0,F);
P3 = P3 *10^3;
T3 = Tc - DSc;
H3 = refpropm('H','T',T3,'P',P3*10^-3,F);

% Point 2
P2 = P3;
T2 = refpropm('T','P',P2*10^-3,'S',S6,F);
H2 = refpropm('H','T',T2,'P',P2*10^-3,F);

% Point 5
P5 = P6;
H5 = H3;
T5 = refpropm('T','P',P5*10^-3,'H',H5,F);

% COP CALCULATION

% Ref. Mass flow rate
mp = CC/(H6-H5); % Kg/s

% Heat / Work Input by Comp.
WD_comp = mp*(H2-H6); % W

% Heat rejected by Cond.
WD_cond = mp*(H2-H3);

% COP
COPm_2 = CC/(WD_comp);
COPt_2 = CC/(WD_comp);
```